THE PEOPLE'S DEMOCRATIC REPUBLIC AND POPULAR

The MINISTRY OF HIGHER EDUCATION AND SCIENTIFIC RESEARCH

UNIVERSITE MOHAMED BOUDIAF - M'SILA

FACULTY : TECHNOLOGY

DEPARTMENT : ELECTRONIC

N° : .....

DOMAIN : SCIENCE AND TECHNOLOGY

FILIERE : ELECTRICAL ENGINEERING

OPTION : D.C.S

Dissertation presented to obtain
The degree of Master Academic

By : BOUAFIA HANANE
OUALI KARIMA

Title

STUDY AND DESIGN OF A RECONFIGURABLE ANTENNA WITH EBG STRUCTURE

Supported in front of the jury composed of:

First and last name Teacher	University	President
.....	University	Rapporteur
.....	University	Examine

Academic year: 2021/2022

THANKS

*First and foremost, we would like to praise **Allah**, the most Gracious and the most Merciful for his blessing given to us during our study.*

*We **BOUAFIA Hanane** and **OUALI Karima** extend our sincere thanks to the Director of our Master thesis Dr. **Hadi KENANE** for his presence, his encouragement, guidance, advices and continuous support. This master thesis would not have been possible without his invaluable technical vision.*

*We also thank Dr **SAHAD Mohammed** and Dr. **KHALFA Ali** for accepting to evaluate our work.*

Last but not least, our heartfelt thanks also go to the professors of electronic department.

We thank our families for their love, care and support throughout life.

As sisters, we are thankful and proud of each other's.

Thanks to Allah

Dedication

with much love I want to say thanks to my mom Kourichi Hemama and dad Bouafia Deradji for their love,my mother the soul of the soul the lamp of my way , my life , my father my crutch, my Shield in this life. I love you both more than you love me

I dedicate my diploma to my bothers Hassaan and Ammarah and my sister Kadi Samia the wife of my brother Ammarah and their son my love Ahmed Kossay.

my dear grandmother Ma Aïcha and mama fatma,

Kossay you are the next graduate in our family inshallah

Our new baby in the family I love you

My grandmother; lakhlef wardia, and my grandpa; Kourichi Elmesoud, Bouafia Esebtii ALLAH YERHAMHOUM. I love you all

My uncle Ali ALLAH YRHMEK NHEBEK

Much love to all my nanas and my uncles and my cosines

I love my three brids and my cat sisi

My friend and sister, ouali karima. You have given me a bond and love in this life. Thank you for being in my life. I love you and I love Fafouna

Every end has a new beginning

Dedication

After a long wait, the dream came true, and we graduated with sincere hearts full of love and gratitude, despite the circumstances, adversity, and bitterness.

My testimony is dedicated to my dear father, Abdelhak rabi yarhmk. Here I have accomplished what I desired for me, my ideal, my dear father. I'm in love with you. I hope you content in your grave with me.

To my dear mother Samia, the light that guides me and the lamp that never goes out, who has supported me throughout my academic career and who has always been there for me in my life's crises, I love you, Mother; without you, I would not have arrived here.

Thank you for your support and encouragement, Abdelhak, my husband. Jannat Al-Firdaws, my dear daughter, I hope to set an example for you in the future and see you graduate at such a time.

My testimony is dedicated to my dear brother Belkacem, my sisters Khansa and Khawla, Safaa, Marwa, and Yousra, as well as my mother-in-law, father-in-law, and all of their children.

My grandmothers are DJamila and Khaira rebi yarhmkom, my grandfather, Seddik rebi yarhmkom, and the children, Akram, Mahdi, Ali, Mayar DJamila chiraz, Alaa, Yasmine, Mohammad Al-Seddiq, oumnia.

Thank you for your kind words and encouragement.

Content

CONTENT

Chapter II

EBG structure

Conclusions

References

Abbreviations list

RA: Reconfiguranle Antenna

Cst: Computer Simulation Technology.

PIN: Positive Intrinsic Negative Diode.

MEMS: Micro Electro Mechanical System.

RF: Radio Frequency.

EBG: Electromagnetic Band Gap.

Introduction

Introduction

Nowadays, Wireless communication have seen rapid growth. Wireless technology is now everywhere in the world.

Every communication system that transmits or receives electromagnetic information requires antennas. Traditionally, antenna design and performance were optimized for a fixed frequency, radiation, and polarization. On the other hand, modern electrical and wireless communication technologies necessitate small, versatile antennas that can adapt to a variety of operating conditions. Antennas that can be reconfigured are another option (RA),

Engineers, researchers, graduate students, and scientists are all fascinated with reconfigurable antennas because of their enticing features, such as the capacity to modify the frequency, pattern, or polarization of a single antenna structure or shape. Reconfigurable antennas are used in commercial wireless communications, auto motive radar, healthcare applications, and many more innovative uses.

The purpose of this memory is to provide a source for understanding the design and analysis of reconfigurable antennas as they pertain to practical applications

Chapter 1 highlight the reconfigurable antennas in many points so we wanted to start with a basic introduction about reconfigurable antennas and illustrated the differences between frequency, pattern, and polarization reconfiguration.

Chapter 2 includes the EBG structure in the reconfigurable antenna designs.

Chapter 3 reveals that we can make a parametric study on any reconfigurable antenna design which allows us to adjust a few parameters in order to achieve our desired results.

Chapter 4 also highlight the optimization for a better design of reconfigurable antenna.

Chapter I
Reconfigurable antennas

I.1 Background

Antennas are essential components of every wireless communication system (regardless of whether they are at the transmitting or receiving end). They are used to radiate (transmit) or receive electromagnetic (EM) waves and have time invariant features. Antenna engineers have designed various types of antennas for a variety of target applications, including short/long-range communication, sensing, imaging, navigation, mobile devices, and biomedical applications, thanks to the advancement and development of the wireless communication industry over the last few decades. Antennas (such as monopoles/dipoles, log periodic, patch, horn, reflector, lens/dielectric, and waveguide-based antennas) are classified depending on their construction, operation principle, or feeding mechanism. Despite the fact that each of these antenna groups has its own set of advantages and disadvantages, these features aid in determining which one is best for you.

Life activities are undeniably and increasingly relyed on and supported by the variety of wireless connectivity in today's world. The majority of antennas used in today's communication systems or wireless platforms operate in a static or fixed manner (fixed frequency, radiation and polarization)

I.2 Reconfigurable Antennas

I.2.1 Introduction

In both academia and industry, reconfigurable antennas play an essential role in modern microwave and millimeter-wave communication systems. The reconfigurable antennas maximize spectrum utilization by altering their frequency and emission pattern features to meet the needs of the system and the surrounding environment. Many characteristics, such as radiation pattern, frequency, and polarization, or a combination of the three, can be used to reconfigure an antenna.

In this chapter, we will see some definitions of reconfigurable antennas, types reconfiguration, the advantages of reconfigurable antenna.

I.2.2 Overview of Reconfigurable antenna systems

A' reconfigurable antenna' is one that may change its performance characteristics (resonant frequency, radiation pattern, polarization, etc.) by modifying its architecture physically or electrically, according to the IEEE Standard Definitions of Antenna Terms published in 2014. The antenna's fundamental operation mechanism normally interacts with the reconfiguration scheme, which adjusts the antenna's surface current or electric field distribution to provide reversible output characteristics. As a result, antenna layouts that do not have an internal reconfiguration mechanism and are instead controlled by external reconfiguration circuits and/or feeding/matching networks are properly justified.

falling outside the ‘reconfigurable antenna’ family. For instance, the performances of a phased array antenna are basically controlled.

I.2.3 Electrical reconfiguration mechanism

From several antenna design perspectives, the electrical reconfiguration process using lumped components is by far the most promising technology. They're simple to co-planarize, making them highly compatible with planar antenna technology and ensuring overall antenna compactness. This approach on the antenna surface does not require any physical modifications or bulky arrangements. Electrical behavior, impedance variation, and variations in the surface current distribution on the antenna structure are all responsible for reconfiguring antenna characteristics. The first form is an RF switch, such as PIN diodes, radio frequency micro-electro-mechanical systems (RF-MEMS), gallium-arsenide field-effect-transistor (GaAs FET), and so on; the second type is a tunable diode (varactor or variable capacitor) that creates tunable responses.

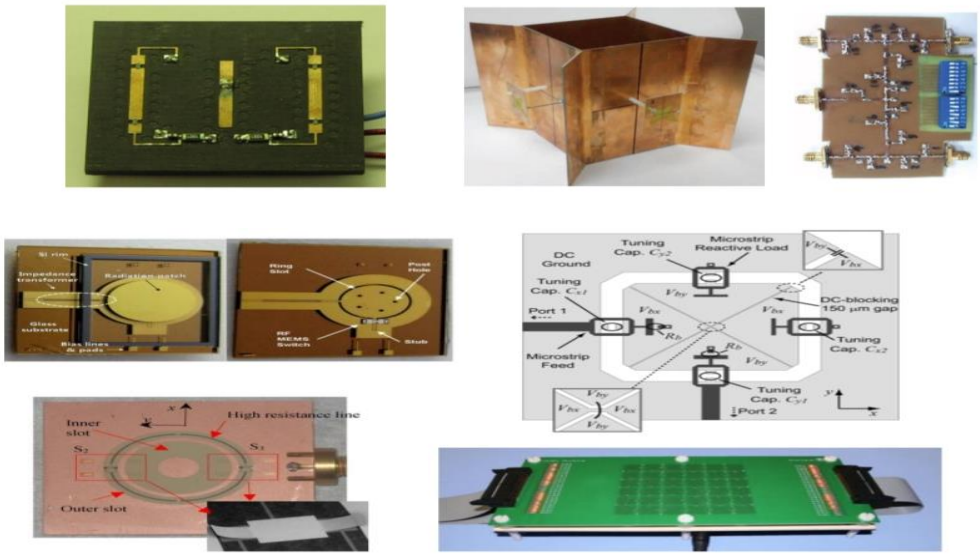

FigureI.1: Electrically reconfigurable antennas: (a) parasitic array controlled with PIN diodes (b) sectoral antenna fed with a switchable power divider, (c) slot ring-stub antenna switched with RF-MEMS, (d) RF-MEMS based annular slot antenna, (e) varactor tuned ring-slot antenna, and (f) switchable pixelated parasitic layer antenna.

I.2.4 Types of reconfigurable antennas

An antenna's reconfigurability is defined as the ability to change its fundamental attributes on purpose. Three essential features of an antenna are required to regulate performance by definition. The reconfigurability of antennas can be divided into four types based on the property that is purposely altered or tweaked.

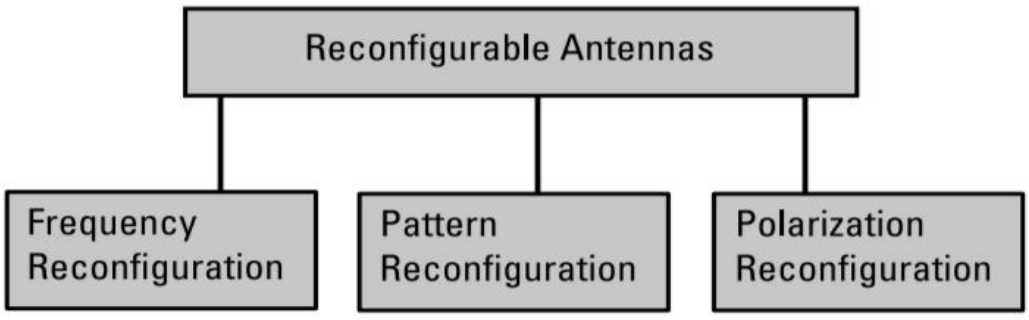

FigureI.2: Typs of Reconfiguration.

I.2.4.1 Frequency Reconfigurability

The most significant property of any antenna is its operation frequency. A frequency reconfigurable antenna is a radiating structure with the capacity to change its operating frequency (or band-notch frequency) within a frequency tuning range.

FigureI.3 depicts a conceptual presentation of tuning the operating frequency of an antenna.

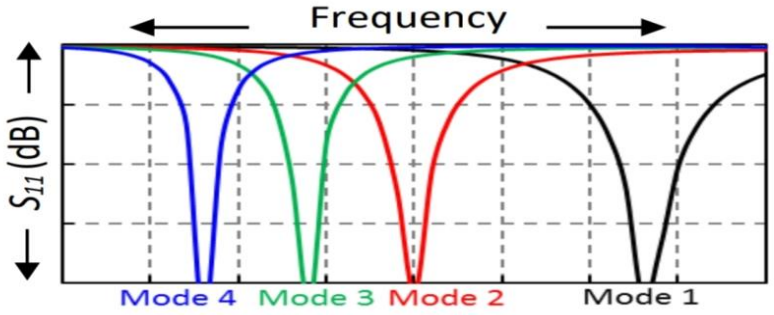

FigureI.3: frequency reconfigurability

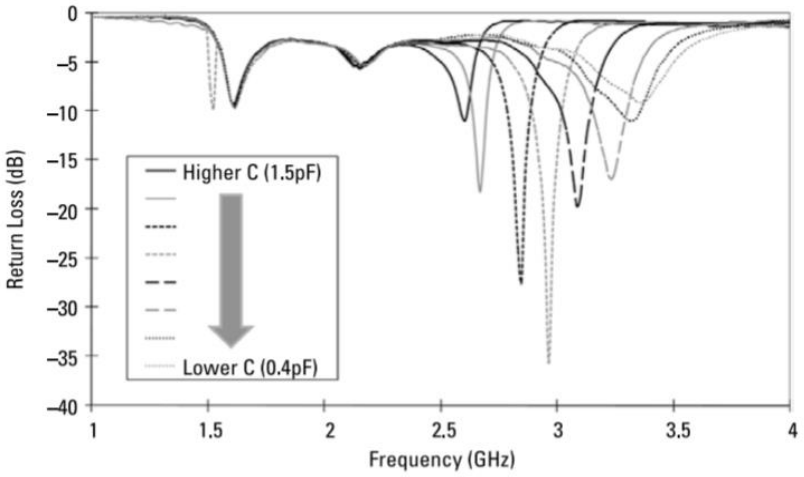

FigureI.4: Measured return loss of the proposed antenna when a different capacitance value is obtained by rotating the trimmer

Generally, frequency reconfigurability can be realized by altering the antenna resonant length physically or electrically through impedance loading, switching, or material property tuning. This type of antenna has the fascinating attribute of frequency selectivity and is excellent for interference filtering because of its dynamic frequency regulating behavior. Thus, frequency reconfigurable antennas have the potential to be promising, cost-effective, and efficient alternatives to multiple FPAs in various scenarios (as currently used in a single device), where multiple single-band antennas are used separately or a single wideband antenna is used to cover individual operation of multiple bands.

Frequency reconfiguration is the process of tuning an antenna to its resonant/operating frequency for a given frequency band. Using the appropriate switching element, it may operate in many frequency bands at a high operating frequency (PIN diode, Varactor diode).

I.2.4.2 polarization reconfigurability

The second category of RA is the polarization reconfigurable antenna,

The polarization mode of an antenna is usually determined by the orientation of its electric field in the propagation direction. A polarization reconfigurable antenna is one that has the capacity to flip between different polarization modes. This antenna can change its polarization mode from horizontal to vertical, linear to circular, or left to right circular polarization, among other things.

FigureI.5 illustrates the concept of polarization reconfigurability.

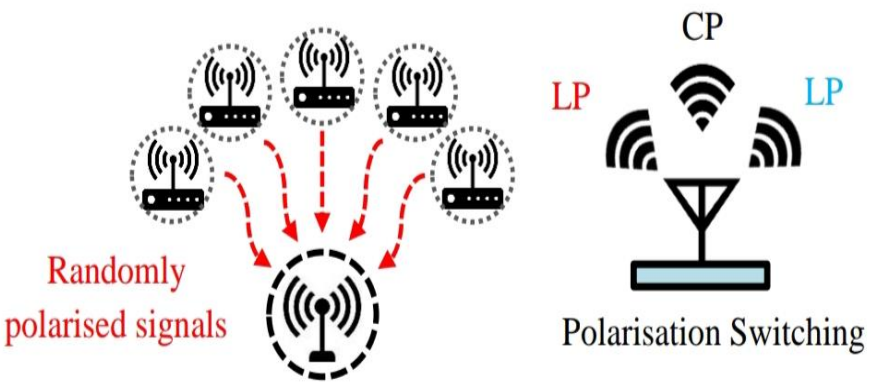

FigureI.5: polarization reconfiguration

Controlled alterations of the antenna configuration, feed arrangement, and/or material property can all be used to produce polarization reconfigurability. Polarization reconfiguration reduces polarization mismatch loss, protects against interfering signals, and ensures excellent signal reception for portable devices.

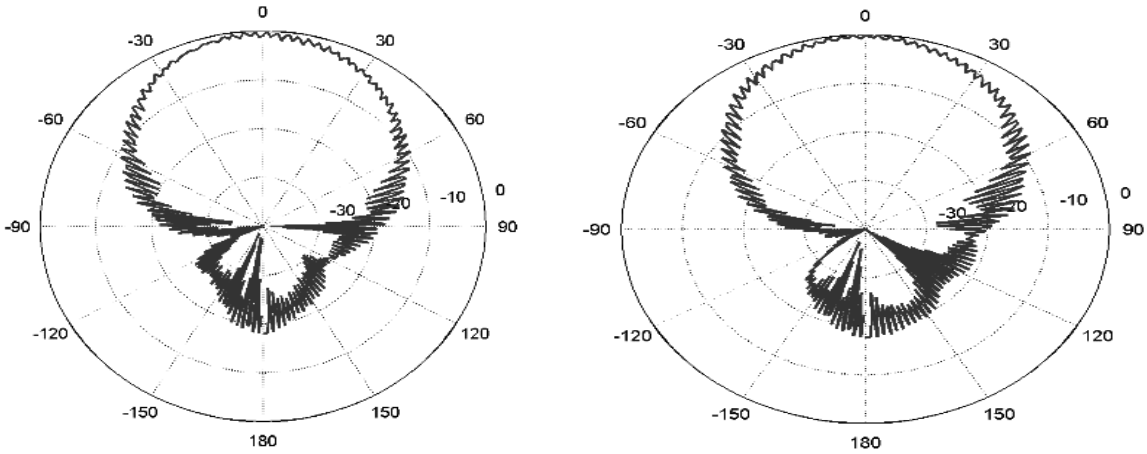

FigureI.6: Measured spinning linear radiation patterns of a circularly polarized stacked microstrip patch antenna

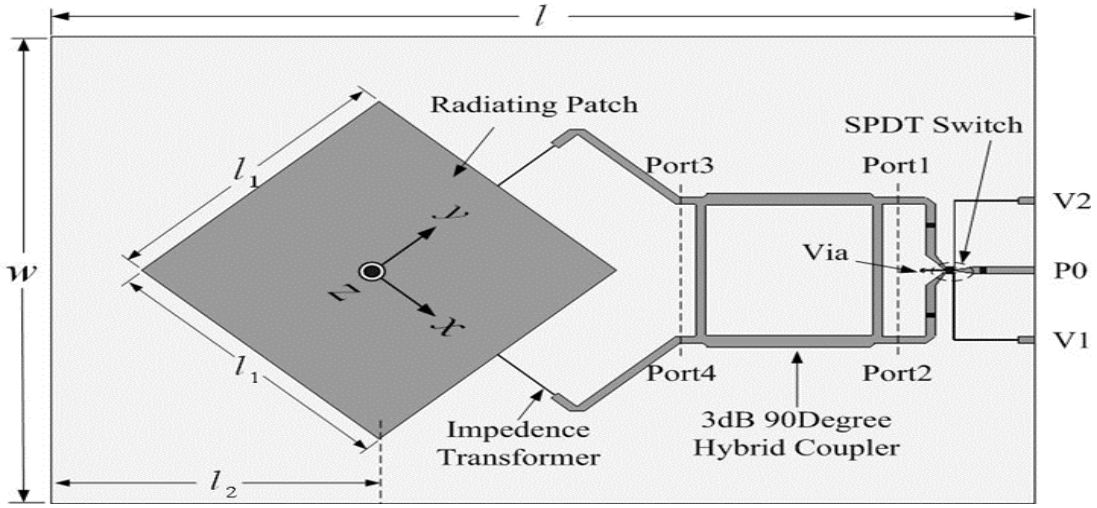

FigureI.7: Reconfigurable Microstrip patch antenna with switchable polarization

TableI.1: Different Polarization States of the Reconfigurable Antenna

	PIN Diodes in Group A	PIN Diodes in Group B	Polarization	Active Varactor Diodes
State I	Forward-biased	Reverse-biased	*x*-oriented	Group B
State II	Reverse-biased	Forward-biased	*y*-oriented	Group A
State III	Reverse-biased	Reverse-biased	45°-oriented	Groups A and B

I.2.4.3 pattern reconfigurability

The pattern reconfigurable antennas belong to the third RA group, which allows them to control their radiation characteristics. The radiation pattern reconfigurable antennas have a great potential to meet the ever-changing requirements of many wireless applications such as cellular and satellite communications, radar systems, vehicle-to-vehicle communication, tracking and remote sensing, on-the-go communication, and so on, thanks to this ability.

Pattern reconfigurable antennas are commonly used for beam steering and null scanning to reduce interference.

PIN diodes, Varactor diode and MEMS are used to change antenna radiation performance.

FigureI.8 shows an application scenario of beam-steering antennas to communicate with portable devices.

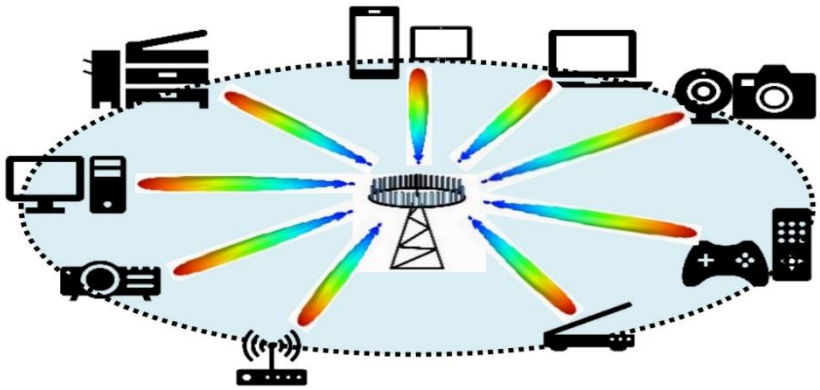

(a)

FigureI.8: Application scenarios of pattern reconfigurable antennas; (a) beam-scanning

Beam-scanning (or beam-steering) antennas provide high gain radiation in the desired direction, allowing mobile and stationary wireless devices to maintain a strong and reliable line-of-sight (LOS) communication link.

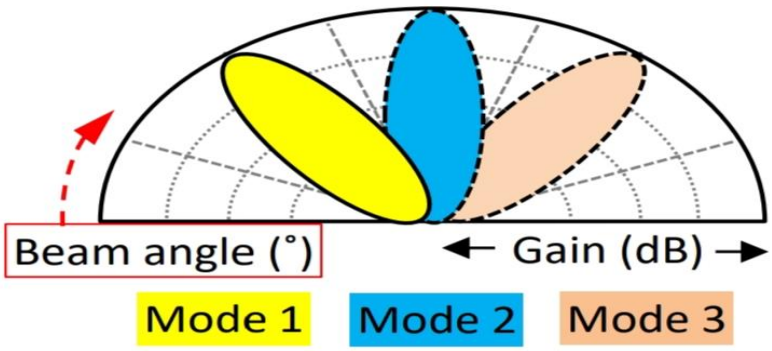

FigureI.9: pattern reconfigurability

The spherical distribution of an antenna's radiation (i.e. spatial far-field radiation) is purposely adjusted to achieve pattern reconfigurability by adapting movable structures, reactive-loading, and switchable parasitic elements.

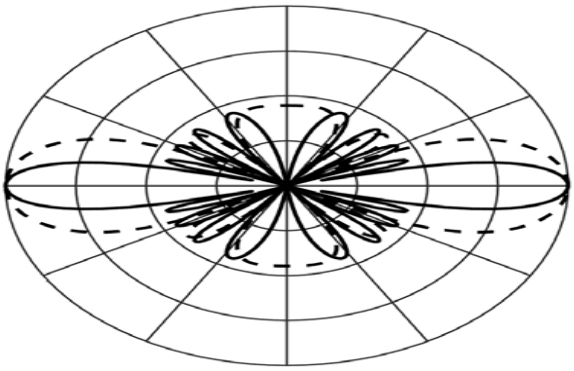

FigureI.10: Normalized radiation patterns of a 10-element linear Dolph-Chebyshev array of isotropic elements; the amplitude taper reflects –22-dB SLL. The solid line indicates elementto-element spacing of 0.5λ, and the dashed line indicates element-to-element spacing of 0.25λ

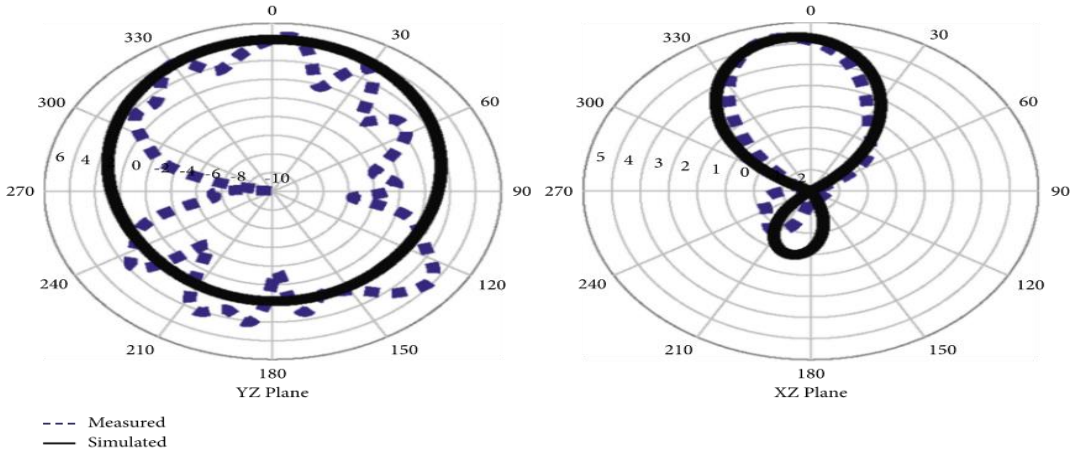

FigureI.11: Radiation pattern recpnfigurable antenna for loT Devices

I.2.4.4 compound reconfigurability

Compound reconfigurable antennas are the last type of RA. They can be reconfigured several times with the same antenna shape using different control methods. Compound reconfigurable antennas may alter operating frequency and polarization, as well as scan the radiation beam and modify the resonant frequency. Controlling each of an antenna's characteristics (resonance, radiation, and polarization) separately without causing significant interference with the others is difficult; however, achieving control of multiple parameters makes the antenna more useful and effective in a changing operating environment.

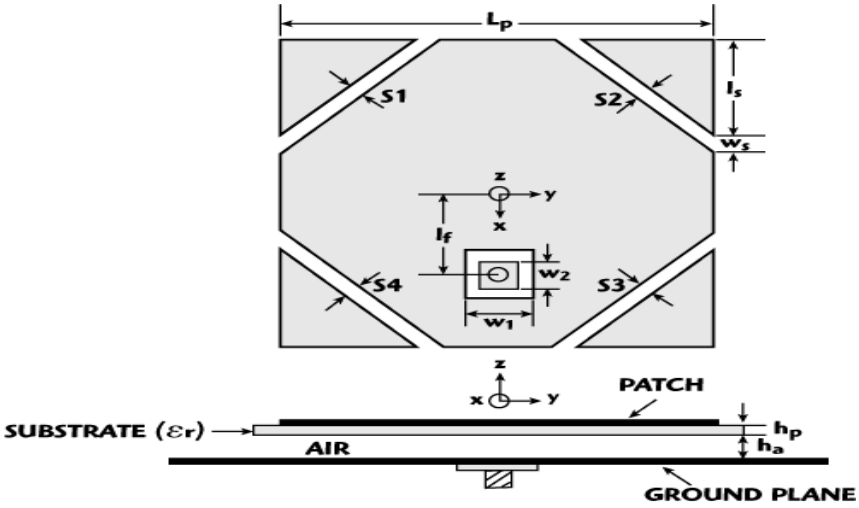

FigureI.12: A Reconfigurable Microstrip Antenna with Frequency and Polarization Diversities

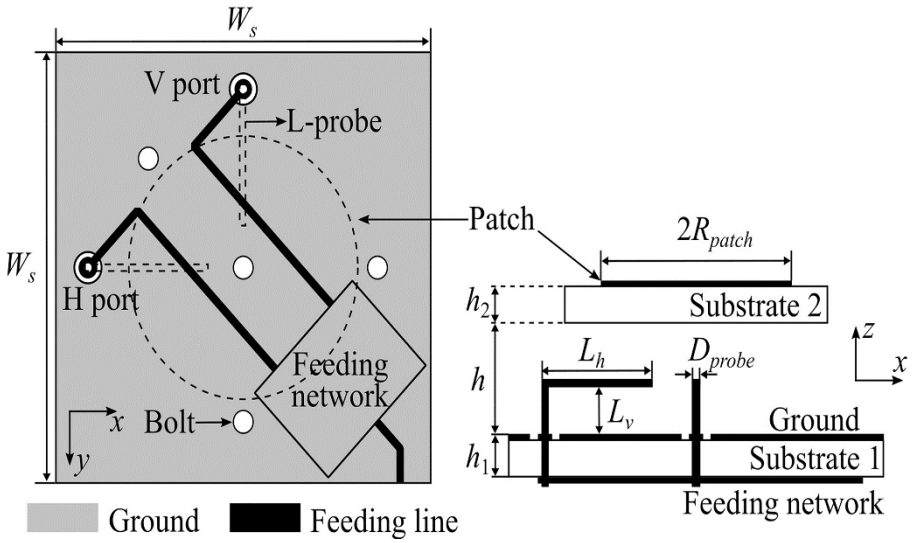

FigureI.13: A quadrature-hybrid-integrated reconfigurable feeding network wideband quad-polarization-agile antenna design

I.3 Advantages of Employing Reconfigurable Antennas

Reconfigurable antennas stand out as an excellent technique for wireless applications from an application standpoint. Because of their dynamic capabilities, flexibility, and contribution to improving system performance, they obviously outperform static type antennas (FPAs). The following are some of the benefits of using reconfigurable antennas:

1) Integrated multi-functionality and adaptability: a) modify antenna functionality as needed by the system; b) function as a single element or a multi-element array; c) compact and low-profile; d) appropriate for narrow band and wideband reconfigurable operation.

2) Support for several wireless protocols: a) cost-effective and space-saving; b) increased selectivity; and d) improved isolation across protocols.

3) Simplified associated feed-circuitry and ease of control; and d) easy and simple integration: a single RA element replaces many static-function antennas (FPAs); b) decreased number of antenna; c) simplified associated feed-circuitry and ease of control; and d) easy and simple integration.

4) Improved system performance: a) strong interference rejection; b) higher speed and data capacity; c) improved communication link efficiency; and d) energy efficiency

5) Front-end processing is minimal: a) interference-suppression techniques are simplified and integrated; and b) the front-end filtering process can be decreased.

6) Software-defined radio (SDR) systems have potential: a) the ability to learn from and adapt to changing circumstances; b) automated control via a controller unit using software intelligence.

I.4 Conclusion

Chapter 1 presents a brief introduction about reconfigurable antennas. An overview, including types of reconfiguration, mechanism, the advantages of implementing reconfigurable antennas are also highlighted. Reconfigurable antennas with EBG structure are so sublime and our next chapter highlight “Electromagnetic Band Gap” EBG structure.

Chapter II
EBG Structures

II.1 introduction

Nowadays, Communication system seen rapidly growing, and antennas are a very important part of them.

Electromagnetic band gap structures help in creating a gap in the band around the operating frequency of the antenna. Popular EBG structures are mushroom-like EBG, polygonal, circular, and spiral.

In this chapter, we will highlight EBG structure (characterization, their reflection phase, …)

II.2 EBG structure

Electromagnetic Band Gap (EBG) structures are a type of artificial periodic structures that encompass a wide range of applications in various antennas and have sparked a lot of interest in electromagnetic research. EBG structures are a new type of artificially produced structure that can control electromagnetic wave propagation within them. These structures possess two distinct electromagnetic characteristics. The first is surface wave suppression in a certain frequency band, known as the band gap. The other is phase response to plane wave illumination; these structures have a reflection phase that varies from 180o to -180o as a function of frequency. Furthermore, these structures have certain interesting characteristics, such as a high impedance in their performance band. A vast range of properties are based on these qualities.

II.3 Fundamental Behavior of Planar EBG

The planar EBG structure changes the geometry of two adjacent solid planes that are commonly used in multilayer PCBs for power delivery. If one of the two solid planes is etched to obtain a sequence of square patches connected by narrow bridges, the resonant behavior of a cavity formed by these two solid planes can be altered. Figure II.1 shows the resonant behavior of a cavity formed by two adjacent solid power planes in a multilayer PCB. The thin dielectric between the two planes (d < <A, d< < B, d<<2, where? is the wavelength associated with the frequency of interest) on the order of a few mils (hundreds of micrometers) simplifies the solution of the Helmholtz equations, and thus the dispersion relation, leading to the expression in (II.1) for the allowed frequencies associated with the resonant TM modes inside the cavity:

$$f_{Tm_\tau\, mn}=\frac{c}{2\pi\sqrt{\varepsilon_r}}\sqrt{\left(\frac{m\pi}{A}\right)^2+\left(\frac{n\pi}{B}\right)^2} \qquad \text{II.1}$$

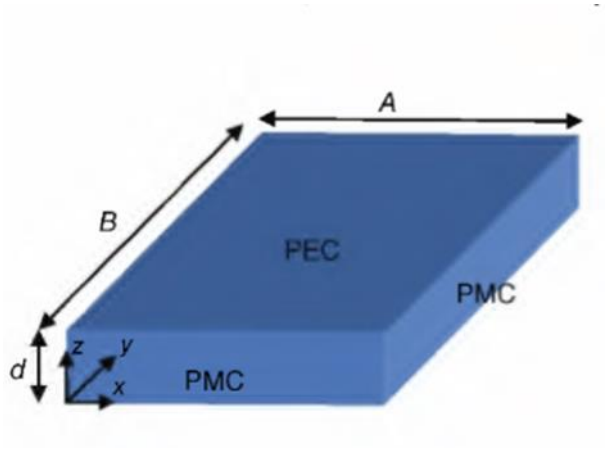

Figure II.1: Top and bottom PEC cavities are ideal

II.4 Reflection Phase

The phase of the reflected electric field at the reflecting surface, and she is the phase difference between the backward and forward waves that formed a standing wave on an arbitrary surface, is an important property of EBG structures.

It varies from 180o to -180o in EBG structures with frequency. As a result, they can be used as proper ground planes in a specific frequency band when the reflection phase is around 0o, similar to Perfect Magnetic Conductors (PMC). An incident wave in the X direction sees a surface in the YZ plane with a surface impedance equal to:

Zs=EZHZ II.2

Furthermore, the surface impedance determines the boundary condition at the surface:

$$E(x) = E_f e^{-jkx} + E_b e^{jkx} \qquad \text{II.3}$$

$$H(x) = E_f e^{-jkx} + E_b e^{jkx} \qquad \text{II.4}$$

$$\frac{E_{totale}(x=0)}{H_{totale}(x=0)} = Z_S \qquad \text{II.5}$$

Moreover, the electric and magnetic fields of each wave are related by means of the impedance of free space as:

$$\left|\frac{E_f(x)}{H_f(x)}\right|=\left|\frac{E_b(x)}{H_b(x)}\right|=\sqrt{\frac{\mu_0}{\varepsilon_0}}=\eta \qquad \text{II.6}$$

And the reflection phase is equal to:

$$\Phi = \mathrm{Im}\left\{In\left(\frac{E_b}{E_r}\right)\right\} \qquad \text{II.7}$$

Finally, the combination of equation (5), (6) and (7) gives the reflection phase of a surface with resistance Zs:

$$\Phi = \mathrm{Im}\left\{In\left(\frac{Z_s-\eta}{Z_s+\eta}\right)\right\} \qquad \text{II.8}$$

II.5 Surface Waves

Many different explanations exist for surface waves. Surface Plasmons are the optical term for them. Surface currents can also be found at radio frequencies. A solution for waves that decay exponentially away from an insulating interface is one way to derive their properties. Only materials with a non-positive dielectric constant, such as metals, are found to have such waves.

We can also find the same waves by starting from the assumption that the impedance material has an effective ne surface. The surface resistance of metal is determined by the depth of the skin.

Because the depth of penetration of the surface wave is equal to the depth of penetration of the skin, surface waves are nothing more than ordinary surface currents and are good at understanding radio frequencies.

II.5.1 Dielectric Interfaces

Surface waves can occur when two different materials, such as metal and free space, come together. Begin with two materials with different dielectric 1 and 2 to derive the properties of surface waves on a general interface.

As shown in Figure II.2, the surface is in the YZ plane, with material 1 extending in the +X direction and material 2 in the –X direction.

Assume that a wave decays in the +X direction with Decay constant and in the –X direction with Decay constant for it to be bound to the surface. First, consider a TM Surface wave with Ey = 0. In material 1, the electric field takes the following form, with the factor eject implicit.

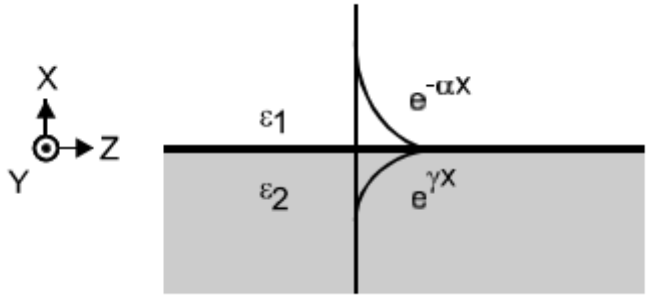

Figure II.2: A surface wave at the interface of two different media

II.6 Effective Medium Model

An Effective medium model can explain many properties of the high-impedance surface. The surface impedance of the structure is set to the impedance of a parallel resonant LC circuit, whose properties are determined by geometry.

When the wavelength is much longer than the size of the individual features, lumped parameters can be used to describe electromagnetic structures. This is also where effective medium theory applies.

The capacitance in this model comes from the overlapping plates in a three-layer design, or from the fringing electric field between adjacent metal plates in a two-layer design. Currents in the ground plane and the top capacitive layer generate inductance. The reflection phase, as well as some of the surface wave properties, can be accurately predicted using this effective circuit model.

II.6.1 Circuit Parameters

A cross-section of the structure is shown in Figure II.3 above. As the structure interacts with electromagnetic waves, currents are induced in the top metal plates a voltage applied parallel to the surface causes charge buildup on the ends of the plates, which can be described as a capacitance. As the charges slosh back and forth, they flow around a long path through the vias and the bottom plate. Associated with these currents is a magnetic field, and thus an inductance. The origin of the capacitance and inductance are illustrated in Figure II .4

Figure II.3: Cross-section of a simple two-layer high-impedance surface

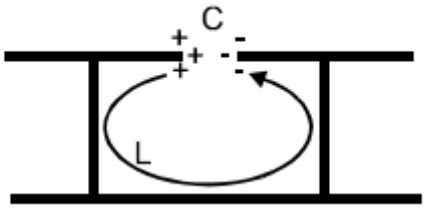

Figure II.4: Origin of the capacitance and inductance in the effective circuit model

The structure's behavior can be reduced to a parallel resonant circuit, as shown. The sheet capacitance and sheet inductance, not the individual element capacitance and inductance, are the appropriate values to use for the model in Figure II.5. These are determined by the value and arrangement of each element.

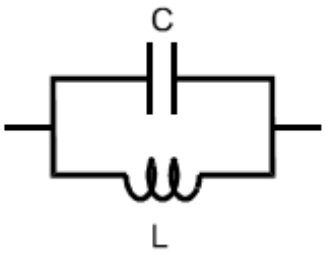

Figure II.5: Modeling the surface impedance with an effective circuit

The fringing capacitance between neighboring co-planar metal plates determines the value of each capacitor in two-layer structures. Conformal mapping, a common technique for solving two-dimensional electrostatic field distributions, can be used to derive this. Figure II.6 shows a solution for a pair of semi-infinite plates separated by a gap, g, with an applied voltage, V.

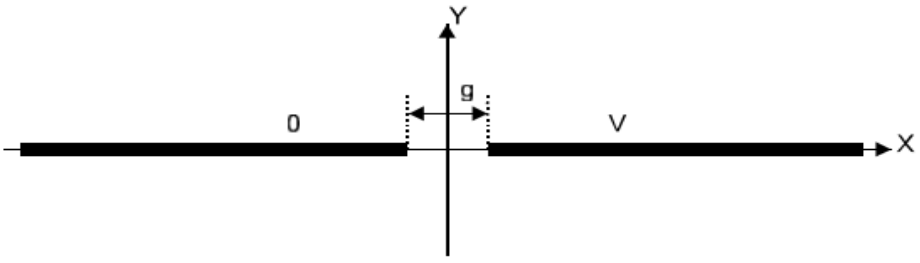

Figure II.6: Capacitor geometry in the two-layer high-impedance surface

The capacitance is infinite, and the field decays nearly logarithmically as you get further away from the gap. The plates, as shown in Figure II.7, end at point a/2 in our geometry.

Ψ= Im [εVcos-1(x+jyg2)] II.9

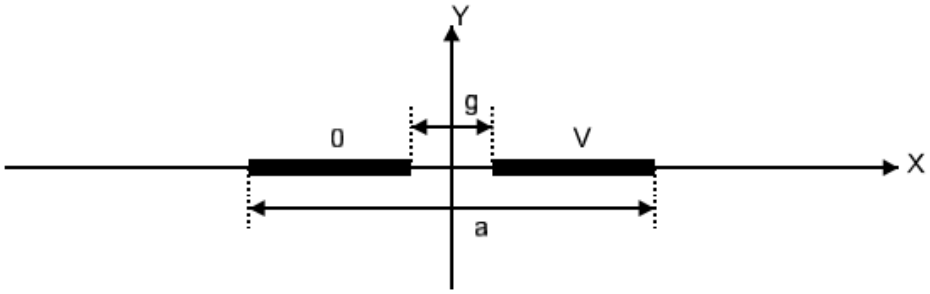

FigureII.7: The geometry of the capacitor in the two-layer high-impedance surface

If a>>g, the capacitance can be calculated by simply terminating Equation II.10 at the plates' ends. The expression below approximates the flux ending on one plate.

$$\Psi = \text{Im}\left[\frac{2\varepsilon V}{\pi} Cos^{-1}\left(\frac{a}{g}\right)\right] = \frac{2\varepsilon V}{\pi} Cosh^{-1}\left(\frac{a}{g}\right) \quad \text{II.10}$$

The capacitance of the three-layer circuit board is calculated using the well-known parallel plate capacitor formula. The overlap area of the plates is A, and they are separated by a dielectric constant ε, distance, d.

$$C = \frac{\varepsilon A}{d} \quad \text{II.11}$$

The product of the individual capacitance and a geometrical factor is the sheet capacitance. A thin slab of dielectric, as shown in Figure II.8, can be used to calculate sheet capacitance. The effective sheet capacitance is determined by applying an electric field tangentially along the slab. The slab can be cut into thin slices of x thickness. We consider the total capacitance in an arbitrary region of length, l, and width, w, of the slab itself.

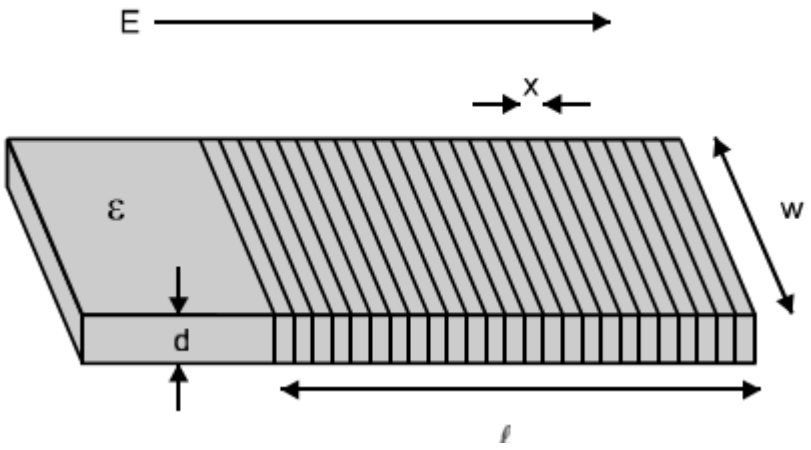

Figure II.8: **A slab of dielectric divided into slices**

II.7 Radiation Bandwidth

On one side, an antenna parallel to the textured surface will see the impedance of free space, and on the other side, the impedance of the ground plane. The antenna current is mirrored by an opposing current in the surface far from the resonance frequency, where the textured surface has low impedance. The nearby conductor shorts out the antenna, resulting in low radiation efficiency. The textured surface has a much higher impedance than free space near resonance, so the antenna does not short out. The radiation efficiency is high in this frequency range.

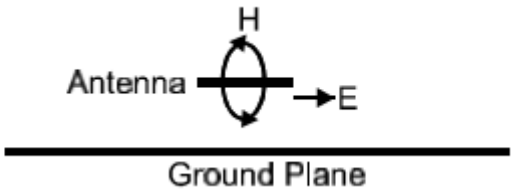

Figure II.9: **A horizontal antenna above a ground plane**

Figure II.9 depicts a horizontal antenna above the ground plane. The antenna is surrounded by a magnetic field, while the electric field runs parallel to it and parallel to the ground plane. Consider the case where the antenna is reduced to a current sheet suspended just above the ground plane.

The antenna current and the image current are superimposed, resulting in electromagnetic radiation.

II.8 Antennas

II.8.1 Patch Antenna

Patch antennas can also benefit from the benefits of surface wave suppression. A patch antenna is a leaky cavity made up of a flat metal shape printed on a dielectric substrate. Metal patches are commonly in the shape of a circle or rectangle, but other shapes are also possible. Low-profile antennas of this type have a narrow bandwidth due to their high resonant nature. A micro strip line on the top surface, a slot in the ground plane beneath the patch, or a coaxial probe can all be used to feed a patch antenna. Figure II.10 shows an example of a patch antenna fed using the coaxial probe method. The probe is placed off-center to excite an asymmetric mode, which radiates more efficiently than the symmetric modes.

Figure II.10: patch antenna on a metal ground plane

Surface waves, like wire monopoles, degrade the patch antenna's radiation pattern. The edges of the ground plane radiate surface waves, which cause ripples in the antenna pattern and backward radiation.

The presence of nearby metal protrusions tends to raise the resonance frequency of the patch, because the effective cavity volume is reduced, as shown in Figure II.11. This can be fixed by leaving a small bare substrate guard ring around the patch or enlarging it.

Figure II.11: A patch antenna embedded in a high-impedance ground plane

Figures II.11 and II.12 illustrate the radiation patterns of the two antennas. At 13.5 GHz, the two antennas have the same return loss. The patch on the ordinary, metal ground plane shows significant backward radiation and ripples in the H-plane and E-plane, respectively. The pattern is not rotationally symmetric, and the H-plane version is much thinner than the E-plane version. The patch on the high-impedance ground plane, on the other hand, produces a smooth, symmetric pattern with minimal

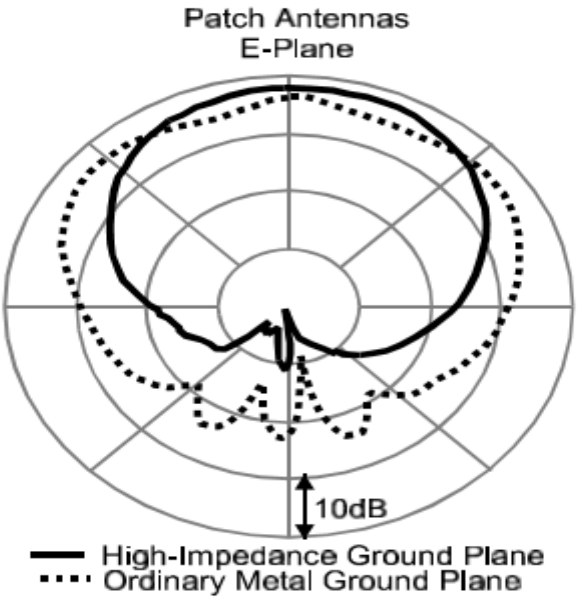

Figure II.12: **E-plane radiation patterns of two patch antennas**

The patch antenna and the high-impedance ground plane are both highly resonant and radiating structures. The patch antenna's frequency and bandwidth can be expressed in the same way we did for the high-impedance surface earlier.

Begin with Figure II.13's patch.

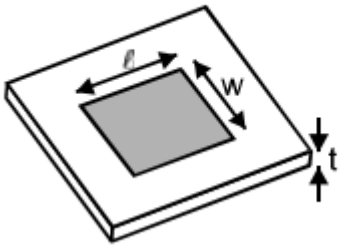

Figure II.13: **Patch antenna**

II.8.2 Circular Polarization

Circular polarization can be beneficial in some situations. Circular polarization, for example, is used in terrestrial moon communications because it allows the receiver to have any orientation with respect to the transmitter. A straightforward procedure for Using a circular wire parallel to the height will produce roughly circular polarization. Figure II.14 shows the ground plane of the resistance.

The wire has a circumference of approximately one wavelength and is fed at one end. The wire's other end is usually left open, but it can also be shortened to the ground for similar results.

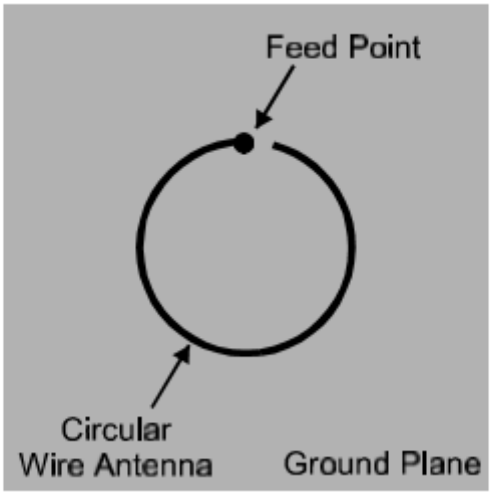

Figure II.14: A circular wire antenna on a high-impedance ground plane.

II.9 EBG Structures Design and Characterization

II.9.1 Mushroom-Like EBG

II.9.1.1 Definition

One of the most basic and common EBG structures is the mushroom-like EBG structure. Figure II.15 illustrates this structure. It's made up of a flat metal sheet with an array of metal protrusions on a dielectric substrate that are connected to the lower conducting surface via metal vias.

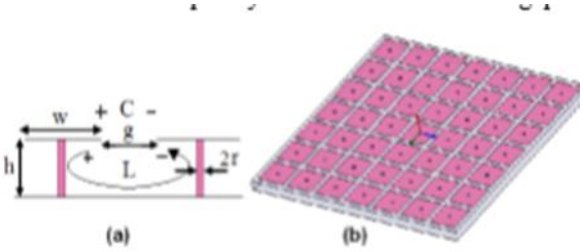

Figure II.15: Mushroom-like EBG, a) unit cell, b) 3D view

II.9.1.2 Parameters of the Mushroom-like EBG

Patch width w, gap width g, substrate thickness h, dielectric constant r, and vias radius r are the parameters of the EBG structure. When the structure's periodicity, which equals w+g, is small in comparison to the operating wavelength, the structure's operation mechanism can be explained using an effective medium model with equivalent lumped LC elements, as explained in. Due to current flowing along adjacent patches, the capacitor C results from the gap effect between the patches and the inductor L. As a parallel resonant circuit, the surface impedance and central frequency of the band gap are calculated.

$$Z=\frac{jwl}{1-\omega^2 LC} \qquad \text{II.12}$$

$$\omega o=1/\sqrt{lc} \qquad \text{II.13}$$

II.9.2 Slot Loaded EBG

As far as slots are concerned, EBG is a new type of EBG structure created by making slots in traditional EBG mushroom-like mineral patches. The current flow on the patches is changed by these openings, which results in a longer current path. It also adds capacity to the space between the slots' edges.

As a result, L and C values are increased, resulting in a smaller frequency band gap and a more compact structure. By cutting a pair of I-like, X-oriented holes in a mushroom-like EBG cell patch, we created a new hole-loaded EBG architecture. The basic mushroom-like cell has the following dimensions: 3mm width, 0.5mm thickness, 1mm height, 0.125mm radius the substrate was an insulating layer with an r of 2.33. The lengths of the slots were then increased to achieve the most compact structure possible. Finally, the holes' dimensions are calculated as follows: L1 is 1.5 mm, L2 is 1 mm, L3 is 0.5 mm, and L4 is 0.25 mm in length. The mushroom-like EBG structure's initial inductance and capacitance are:

$$C = \frac{\mu_0 \mu_r h}{\pi} cosh^{-1}\left(\frac{W+g}{g}\right) \quad \text{II.14}$$

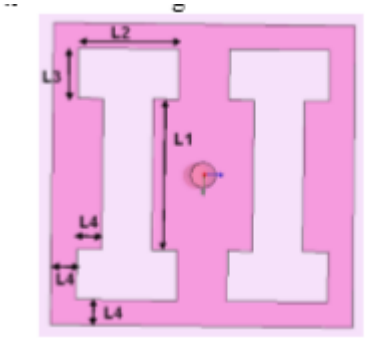

Figure II.16: Unit cell of the designed EBG cell

II.9.3 Characterization of EBG Structures

II.9.3.1 Reflection Phase Diagram

One of the most important features of EBG structures is their reflection phase. A unit cell is modeled in HFSS, and periodic boundary conditions on side walls are applied to extract the reflection phase diagram. A plane wave at various frequencies excites the cell, and the phase of the reflected wave at the evaluation plane is calculated as:

$$\Phi_{EBG} = \frac{\int_s Phase(E_{scattered})ds}{\int_s sds} \quad \text{II.15}$$

S is the evaluation plane.

This method yields the reflection phase diagrams of a normally incident plane wave on the traditional mushroom-like EBG and the new slot loaded EBG, as shown in Figure II.17

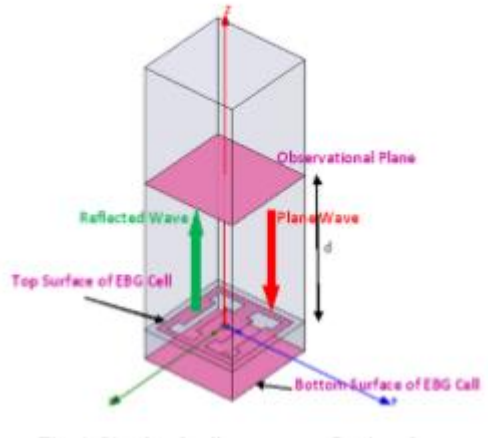

Figure II.17: Simulated cell to extract reflection phase

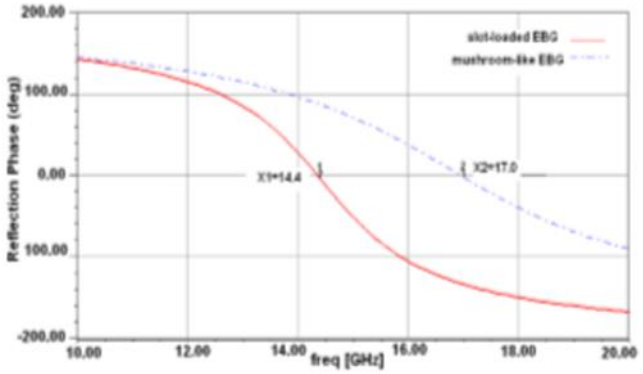

Figure II.18: Reflection phase of a normally incident plane wave with Ex polarization on the two types of EBG structures

II.9.3.2 Dispersion Diagram Method

The Dispersion diagram, also known as the -f curve, is another important feature of EBG structures that can be calculated using the unit cell and a periodic boundary condition with appropriate phase shifts on the sides.

The dispersion curve is periodic, according to the Floquet theorem and its expansion by Bloch. As a result, we only need to plot the dispersion relation over a single period, referred to as the Brillouin zone. The irreducible Brillouin zone is the smallest region within the Brillouin zone where the directions are not related by symmetry. Our structure's irreducible Brillouin zone is a triangular wedge with 1/8 the area of the full Brillouin zone defined by, and M points the CST Microwave Studio simulated cell**.**

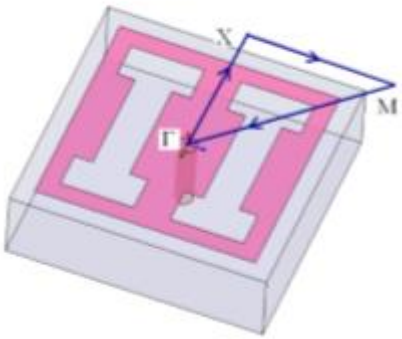

Figure II.19: The simulated cell to extract dispersion diagram.

II.9.3.3 Direct Transmission Method

Direct transmission is another method for determining the band gap of an EBG structure. The scattering parameter S21 is used to model wave transmission through the EBG structure in this method. A TEM waveguide with two pairs of parallel PEC and PMC sides, as shown in Figure II.20, is a part of structure that is repeated in different directions of the lattice.

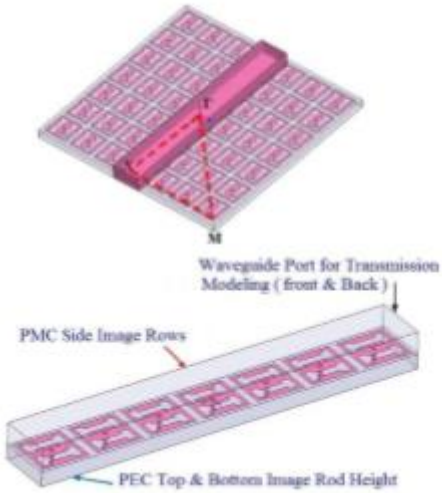

Figure II.20: The simulated TEM waveguide in direct transmission method.

II.10 Application Examples

II.10.1 Splitting Power Planes by EBG Barrier

The EBG's most common applications are for the layout of a complete plane. Other layout constraints, on the other hand, may limit the EBG design on the entire plane. The example presented here shows how the EBG can be designed only on a small plane section, allowing it to be freely laid out where it is most useful without affecting other system functions. As shown in Figure II.21, this application example of the EBG geometry is aimed at isolating two sections of the PCB, Area 1 and Area 2, where two high-speed ICs, IC, and IC, are located. These ICs produce high-speed digital signals at a data rate of 10 GB/s, taking into account the possibility of noise from a band centered at the data rate fundamental harmonie, 5 GHz. The overall board's important geometry features are shown in. It has a dielectric permittivity of r=4.4 and is 0.4 mm thick between the two metal planes.

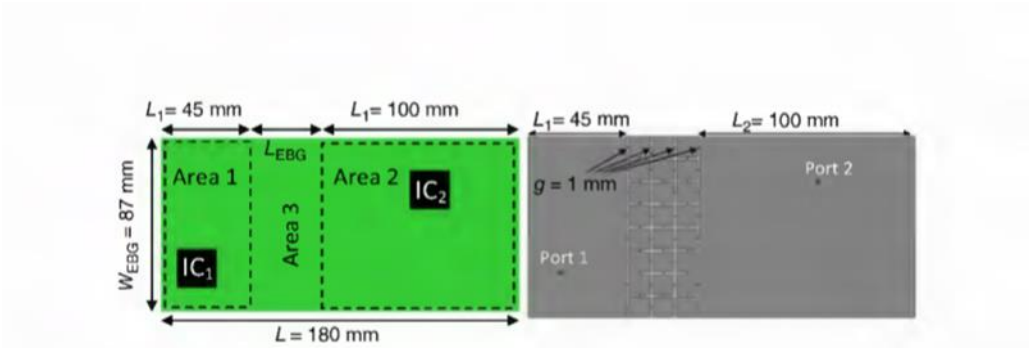

(a) **(b)**

Figure II.21: (a) Geometry of the two-layer PCB considered in the example. (b) Design of the 3 x 8 EBG to fit the unconstrained Area 3

II.10.2 IC Isolation by an EBG Fence

As a second application example, a multilayer PCB with several high-speed ICs is shown. The first harmonie is at 5 GHz, and one of the ICs operates at 10 Gbps. Because the noise generated by this ICc can propagate within the power planes, it must be reduced over a wide frequency range that includes, at the very least, the 5 GHz fundamental harmonie. As shown in Figure 2.5a, the PCB area of interest is centered on the IC location, where the PCB excitation port is located. The IC outline with a side length of 30 mm is identified by the dashed line. The study looked at a total PCB area of 80 mm X 80 mm.

A multilayer PCB with several high-speed ICs is shown as a second application example. One of the ICs operates at 10 Gbps, and the first harmonie is at 5 GHz. Because the noise generated by this ICc can travel through the power planes, it must be reduced over a broad frequency range, at the very least the 5 GHz fundamental harmonie. The PCB area of interest is centered on the IC location, where the PCB excitation port is located, as shown in Figure 2.5a. The dashed line marks the IC outline with a side length of 30 mm. A total PCB area of 80 mm X 80 mm was studied. An optional port location is considered (Port I') to evaluate the effect of the distance between the source and receiving port when divided by the same EBG fence. The stack-up needed for the EBG design consists of two metal layers embedding a 0.2 mm dielectric characterized by r=4.4.

To place four equal planar EBG structures, Area 2 is divided into four parts (Parts 1-4). The EBG is designed in accordance with the procedure's quick and efficient details. According to the first resonant mode TM 10the single patch, the size and of the EBG patch fixes the band gap upper limiting.

II.11 conclusion

Chapter 2 presents EBG structure. Fundamental behavior of planar EBG, reflection phase, surface waves, Effective medium model, radiation bandwidth, antennas, EBG design and characterization, there are also application Examples. Our next chapter highlight the simulation of an antennas with and without EBG structure in many models.

Chapter III
Parametric study of an EBG antenna

III.1 Introduction

In the field of electronics, especially in wireless telecommunications, where recent development offers a new perspective and sophisticated means such as reconfigurable antennas and their importance in improving daily life, the evolution and technological development makes a radical change**.**

In this chapter, we'll perform a parametric analysis to see how different geometric (dimensions) and physical (substrate, etc.) parameters affect the reconfigurable antenna's adaptation. A parametric study will be performed to see how these settings affect the characteristics of the designed antenna (operational frequency, radiation pattern, and bandwidth).

III.2 Choice of simulation tool

There are several electromagnetic simulators specifically designed for the design of microwave components (printed antennas, HF filters, etc.). HFSS, ADS Momentum, IE3D, FEKO, and CST MICROWAVE STUDIO are some of these simulators. We will use the CST studio in our study for a simple reason: it is impossible to master all of these tools in a short period of time, and this tool, unlike others like ADS, allows us to design the antenna in 3D. The CST simulator is a specialized tool for three-dimensional electromagnetic simulation and design (3D) high frequency components, which uses the finite integration method to solve Maxwell's equations.

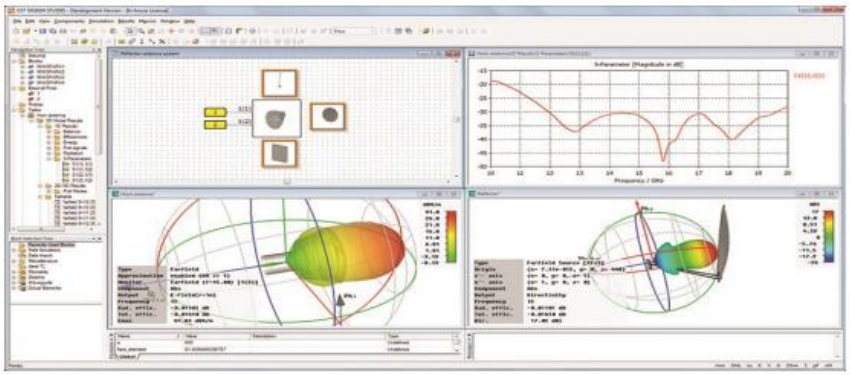

Figure III.1: a graphic interface for the CST studio simulator

The effective dielectric constant is calculated using the formula

$$\varepsilon_{eff} = \left(\frac{\varepsilon_r+1}{2}\right) + = \left(\frac{\varepsilon_r+1}{2}\right)\left(1 + 10\frac{h}{w}^{-\frac{1}{2}}\right) \quad \text{III.1}$$

You must use the CST's impedance calculator for the model that corresponds to antennas fed by a feed line in order to have an impedance adaptation. Wheeler's synthesis equations [32] are used in this calculator. As a result, for a substrate height of h=1.6 mm and an input impedance of 50, a feeder width Wf of 3 mm is required (see Figure III.2)

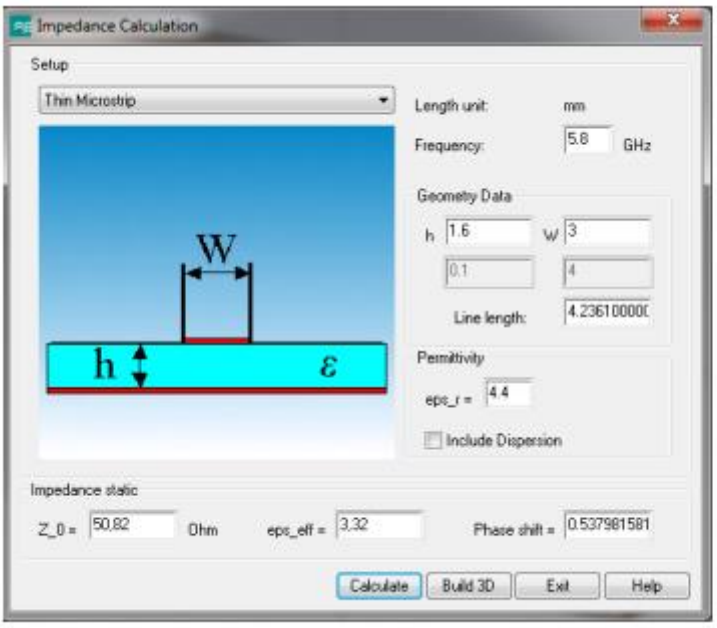

Figure III.2: CST software is used to calculate Zo for given w and ε_r

III.3 Parametric study of a lotus antenna model

During the parametric study, we must vary a single parameter while keeping the other parameters constant, allowing us to isolate the dependence between physical parameters. We will then observe the effect of changing this parameter on the designed antenna's characteristics such as resonant frequency, radiation pattern, and reflection coefficient. Indeed, we want to create a working antenna for the WLAN band (2.4 GHz or 5.8 GHz)

III.3.1 Antenna geometry

We start with a patch antenna in the shape of a lotus flower with a complete ground plane. The proposed antenna is built on a low-cost substrate (FR4) with a width length dimension of 60*52mm² and a relative permittivity of Ɛr 4.3, The copper thickness is 0.035 mm, and the ground plane dimensions are 20*52mm² (length width).

As shown in Figure III.3, the patch is directly connected to the supply line with a characteristic impedance of 50.

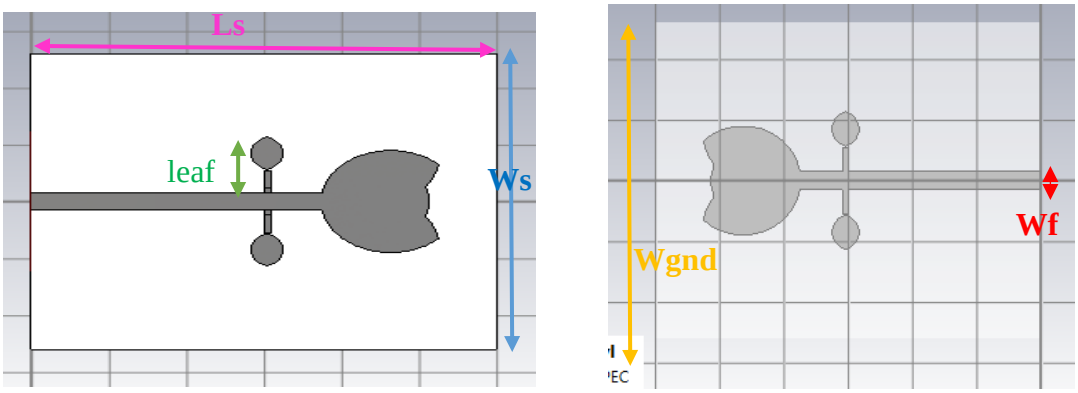

(a) **(b)**

Figure III.3: The rectangular Lotus antenna's geometry;

(a) front view, (b) back view

Table III.1: The dimensions of the proposed antenna in mm

Lgnd	Wgnd	Ls	Ws	L1	L2	L3	Wf	R1	Dx	Dy	XL1	Wh1	Wh2
60	52	60	52	30	2.3	3.7	3	9	1	0.9	30	0.9	0.9

This first simulated structure with the above-mentioned dimensions does not produce interesting results (see Figure III.4). A reliable solution was found in a parametric study of the various previous settings in order to improve the characteristics of this patch antenna.

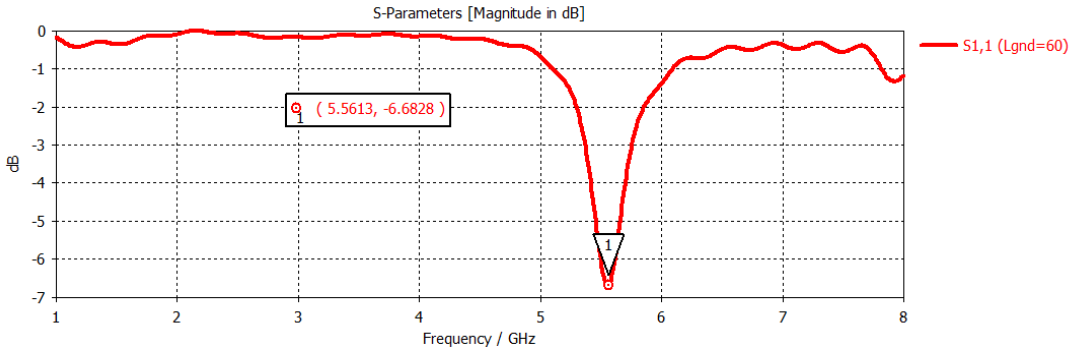

Figure III.4: S1,1 reflection coefficient for the antenna described in Table III.1

Following the simulation, the obtained reflection coefficient shows a minor adaptation on the 5.56 GHz frequency, which is outside of the desired frequency range. The goal is to have a reflection coefficient modulus in the band corresponding to less than -10 dB.

The surface current distribution can usually be measured at a frequency where the reflection coefficient is low (resonant frequency). The socket will be made at the 5.56 GHz frequency, for example, as shown in Figure III.4.

Because of the limitations in this first structure, changes will be made to the radiating patch and mass (fence creation), as well as the alimentation line (insertion of troncatures (cut feeding), and the addition of resonant tiges (stub). Furthermore, the dimensions of various surfaces can be changed independently. All of these changes are aimed at improving the antenna's performance.

III.3.1.1 The Ground Effect (Lgnd)

When its length is reduced to Lgnd = 20 mm and the position of the feed line is adjusted to be under the beveled angle, a beveled rectangular patch antenna with a partial ground plane is used. The feed line in traditional designs is placed in the middle of the rectangular patch, resulting in a uniform current distribution across the patch.

The dimensions used in this step are listed in the table below;

Table III.2: the dimensions of the patch antenna proposed in mm

Lgnd	Wgnd	Ls	Ws	L1	L2	L3	Wf	R1	Dx	Dy	XL1	Wh	Wh2
20	52	60	52	30	2.3	3.7	3	9	1	0.9	30	0.9	0.9

The return loss curves for many ground plane widths (Wgnd) after the parametric study are given in Figure III.5.

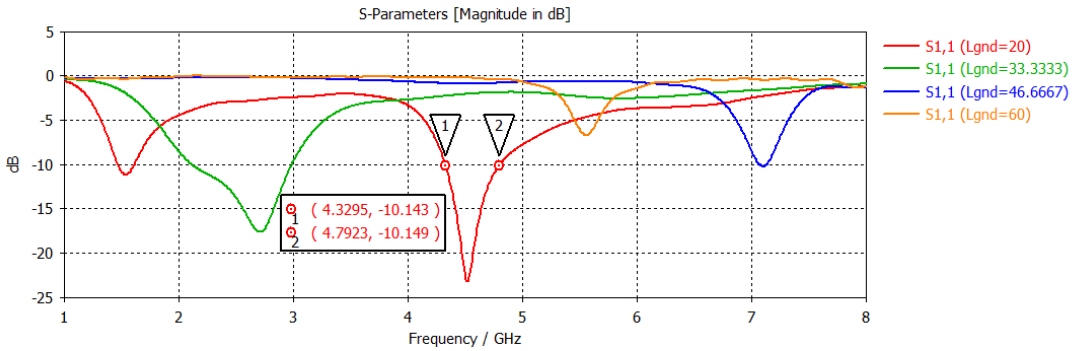

Figure III.5: S1,1 return loss curves for a variety of Lgnd values

Many curves in the band [4.32-4.79 GHz] have low return loss (less than -10 dB), as shown in the diagram above. In terms of bandwidth, the red curve with Lgnd=20 mm is the best.

III.3.1.2 The effect of truncation length (XL1)

while the truncation length (XL1) is varied from 20mm to 30mm. Other variables are set, The simulation results are shown in Figure III.6 as a function of frequency in terms of the reflection coefficient S11.

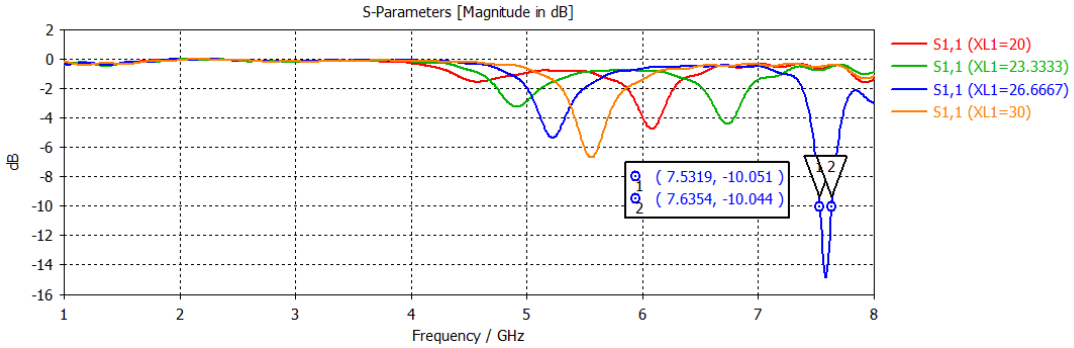

Figure III.6: The reflection coefficient for different truncation lengths XL1

Many curves in the band [7.53-7.63 GHz] have low return loss (less than -10 dB), as shown in the diagram above. In terms of bandwidth, the blue curve with XL1=26.6 mm is the best.

III.3.1.3 The effect of The Switch ON OFF (Wh1, Wh2, XL1)

We'll change the width of the truncation Wh1 and Wh2 from 0 to 0.9 mm and the truncation length XL1 from 20 to 30 while keeping the other parameters constant.

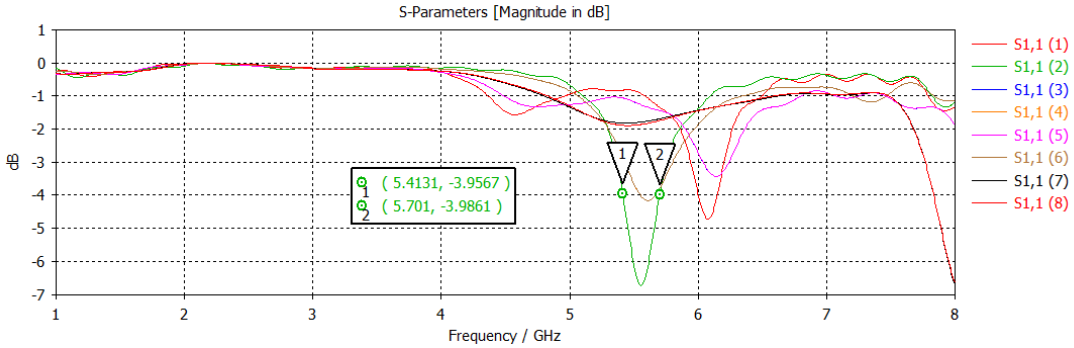

Figure III.7: The reflection coefficient for different truncation lengths XL1 and widht Wh1, Wh2

The result (5.41-5.670 GHz) is not satisfactory, because in the place where I was Switchs there is no current, as shown in Fig 8.III, for this we will not discuss any parametric study.

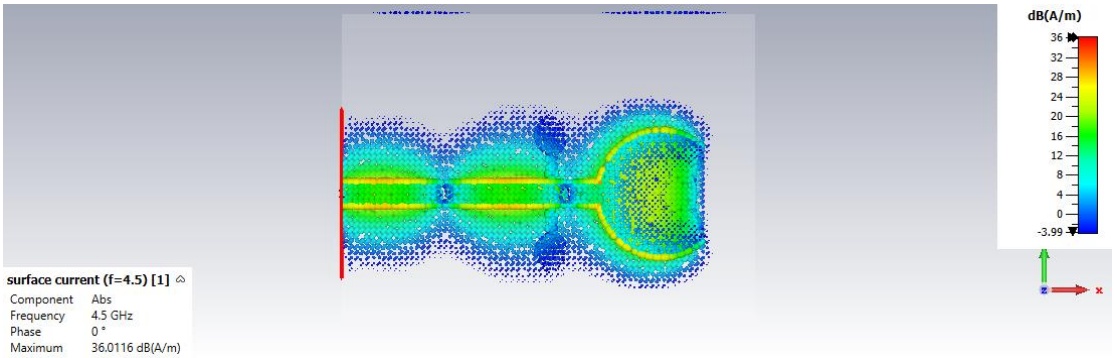

Figure III.8: **The surface current distribution on the antenna at the 4.5 GHz frequency**

III.3.2 Inserting a truncation on the Cylinder's effect (Inset)

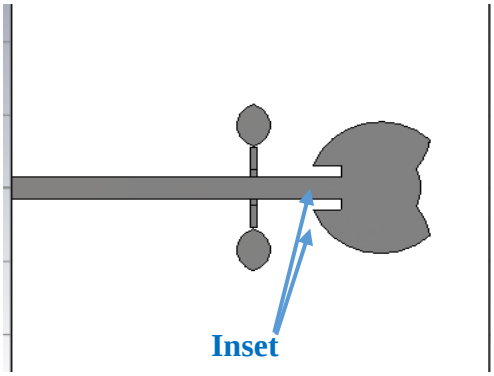

Figure III.9: **Rectangular antenna with inset; front view**

The dimensions used in this step are listed in the table below;

Table III.3: **The dimensions of the patch antenna with inset proposed in mm**

Lgnd	Wgnd	Ls	Ws	L1	L2	L3	Wf	R1	Dx	Dy	XL1	Wh1	Wh2	Y0	G
20	52	60	52	30	2.3	3.7	3	9	1	0.9	30	0.9	0.9	0.9	3

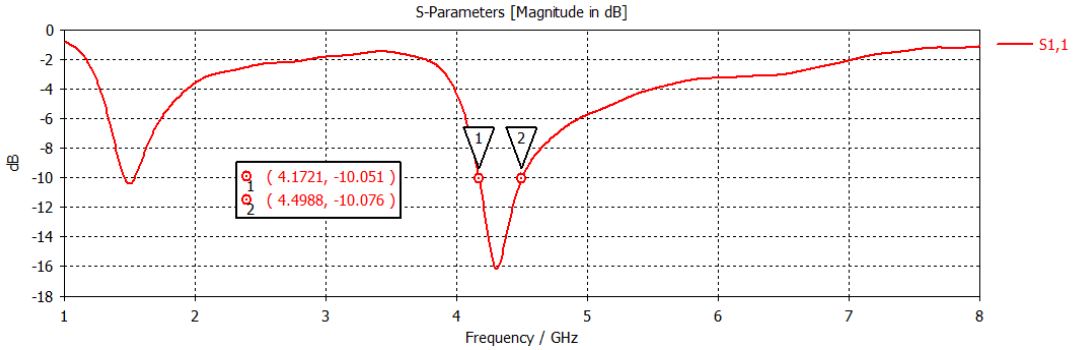

Figure III.10: **The reflection coefficient for inset**

The secends result (4.17-4.49GHz) is satisfactory, but we need to increase the bandwidth. In this step, we'll change the dimensions of the first beveled angle while another beveled angle is present. Using the CST genetic optimization method, the optimization process will be run to obtain the best value for this dimension.

III.3.2.1 The effect of truncation length (yo)

The truncation width g is fixed at 3 mm in this study, while the truncation length (yo) is varied from 0.9mm to 1.5mm. Other variables are set; the simulation results are shown in Figure III.11 as a function of frequency in terms of the reflection coefficient S11.

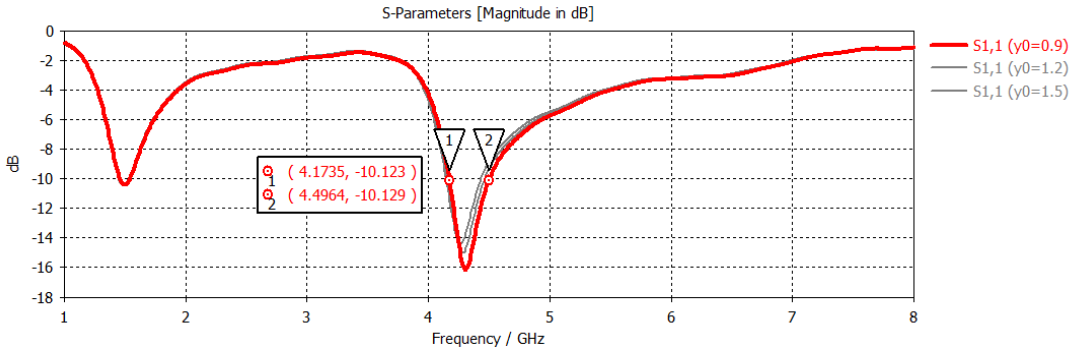

Figure III.11: The reflection coefficient for different truncation lengths yo

We can see that while the length of the yo has no effect on the resonance frequency, it does affect the adaptation. At the (4.17-4.49GHz) frequency, this adaptation reaches its maximum value (-10dB). However, for yo= 1.5mm, it reaches its maximum value at 4.24 GHz.

III.3.2.2 The effect of truncation width (g)

We'll set the truncation length to yo=1.2mm in this section, then change the width of the truncation g from 3 to 5 mm while keeping the other parameters constant.

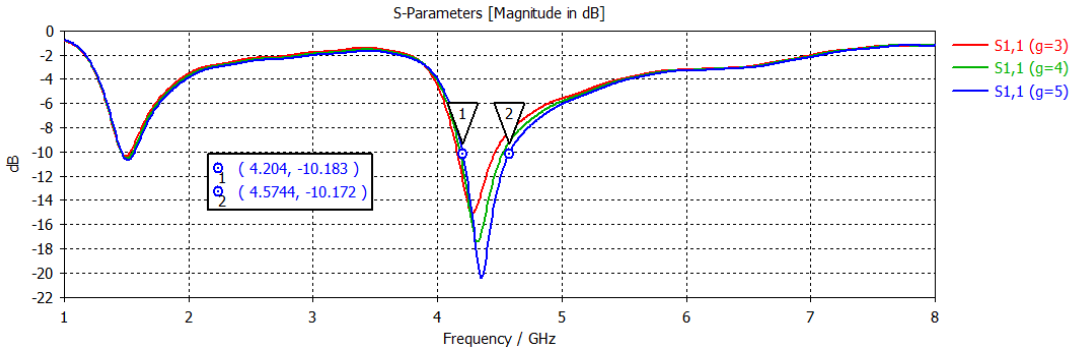

Figure III.12: The reflection coefficient for different truncation widths g

The adaptation on the resonance frequencies (4.42-4.57GHz) affected by the variation of the truncation width, as in the previous case. For a width of g=5mm, there is a better adaptation reaches its maximum value (-20dB)

III.3.3 The slot effect on the patch

Now we'll cut a hole (slot) in the radiant patch to improve the performance of a traditional patch antenna, such as expanding the band bandwidth or creating new resonance frequencies.

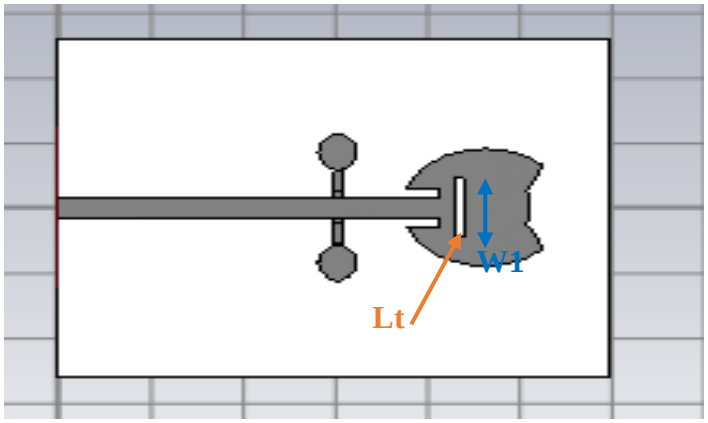

Figure III.13: The dimensions of the hole created on the patch; front view

The dimensions used in this step are listed in the table below;

Table III.4: the dimensions of the patch antenna with inset and Trou proposed in mm

Lgnd	Wgnd	Ls	Ws	L1	L2	L3	Wf	R1	Dx	Dy	Y0	G	Lt	W1
20	52	60	52	30	2.3	3.7	3	9	1	0.9	0.9	3	1	9

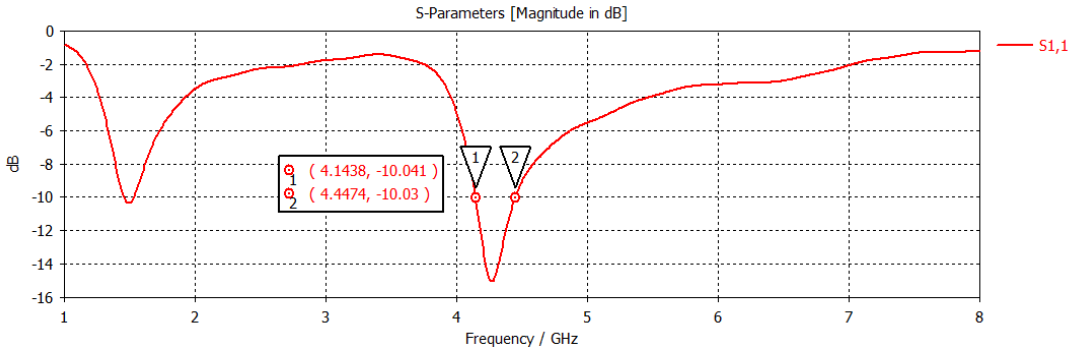

Figure III.14: The dimensions of the hole created on the patch

The secends result (4.14-4.44GHz) is satisfactory, but we need to increase the bandwidth. In this step, we'll change the dimensions of the first beveled angle while another beveled angle is present. Using the CST genetic optimization method, the optimization process will be run to obtain the best value for this dimension.

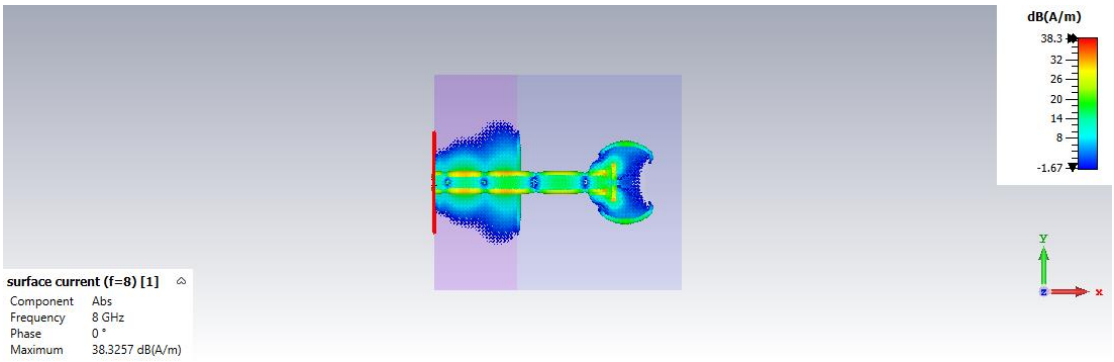

Figure III.15: The surface current distribution on the antenna at the 8GHz frequency

The surface current distribution can generally be measured at a frequency where the reflection coefficient is low (resonance frequency). Figure III.15 shows that the tap will occur at 1 GHz, 4.5 GHz, and even 8 GHz.

In order to find the excitation modes, this distribution provides an idea of the current flow on the radiating surface.

III.3.3.1 The effect of slot width (W1)

In this case, we'll change the slot width (W1) from 3 to 11 mm while keeping the other parameters constant. The slot a length is fixed at 2 mm.

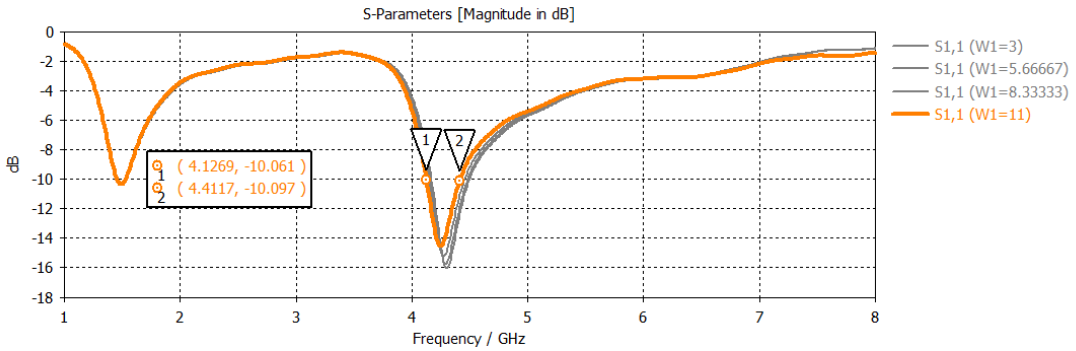

Figure III.16: Evolution of the reflection coefficient in frequencies for different widths of slot W1

The different curves of the modulus S11 in Fig. III.13 show that a hole in the radiated patch can affect the conditioning of the antenna and also create an echo (4.12-4.41 GHz). And we can say that whenever W1 increased We see That the adaptation decreased.

III.3.3.2 The effect of slot length (Lt)

In this experiment, the slot width is set to W1=11 mm, and the length of the slot (a) is varied from 0.2 to 1 mm, while the other parameters remain constant.

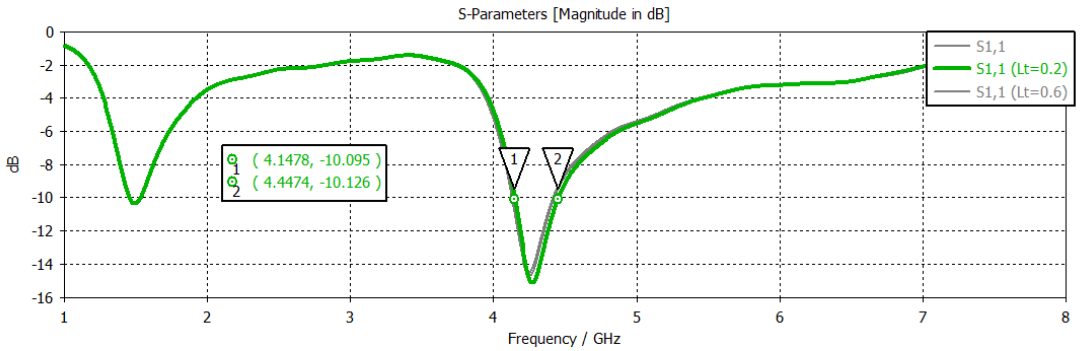

Figure III.17: Evolution of the reflection coefficient as a function of frequency for different slot lengths Lt

The second-step result (4.14-4.44GHz) is satisfactory, is only affected by the variation of the truncation length.

also we can say that whenever Lt increased We see That the adaptation decreased like the past step

III.3.4 Inserting a truncation on the Cylinder's effect

III.3.4.1 Without Inset

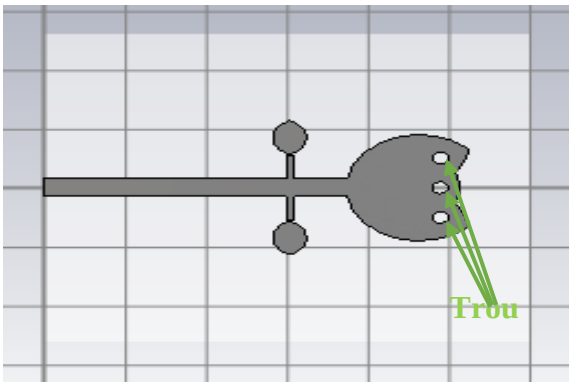

Figure III.18: Rectangular antenna with Truncation on the Cylinder; front view

The dimensions used in this step are listed in the table below;

Table III.5: The dimensions of the patch antenna with trou proposed in mm

Lgnd	Wgnd	Ls	Ws	L1	L2	L3	Wf	R1	Dx	Dy	XL1	Wh1	Wh2	Lcy	Lcy1	d1
20	52	60	52	30	2.3	3.7	3	9	1	0.9	30	0.9	0.9	4	3	1

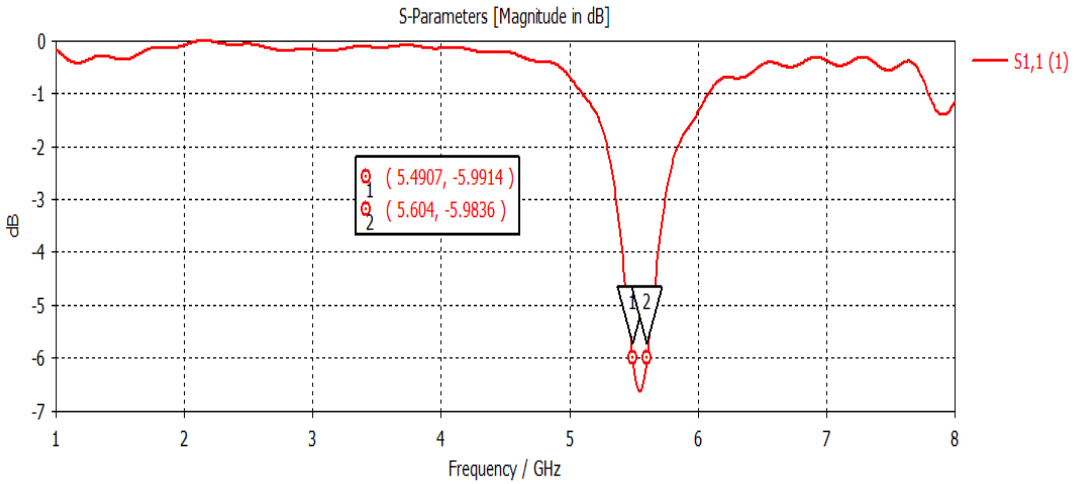

Figure III.19: The reflection coefficient of Rectangular antenna with truncation on the Cylinder

The result (5.49-5.604 GHz) is not satisfactory, because in the place where I was a hole cylinder there is no current, as shown in Fig 15.III, for this we will not discuss any parametric study.

III.3.4.2 With inset

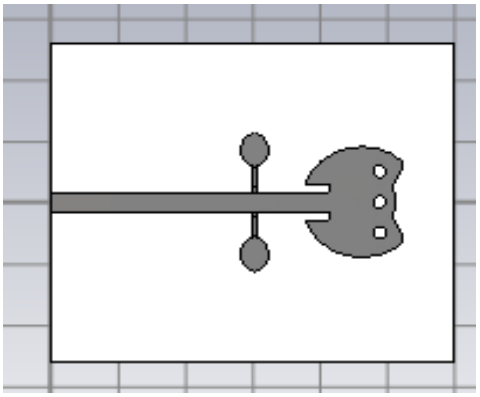

Figure III.20: Rectangular antenna with inset and Truncation on the Cylinder; front view

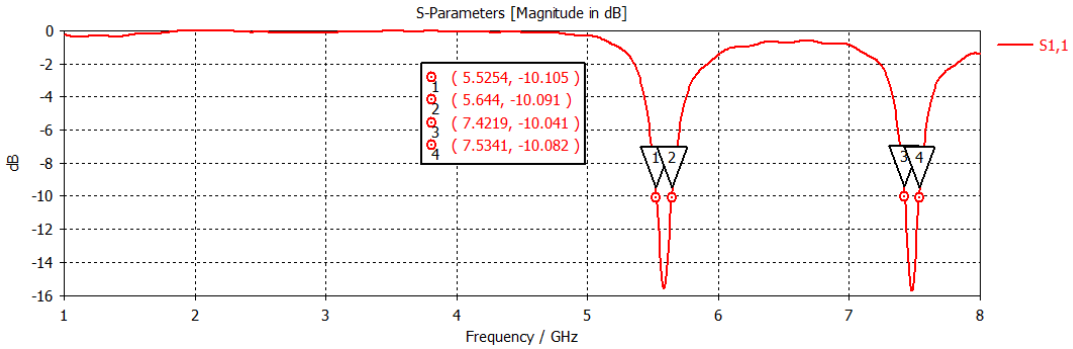

Figure III.21: The reflection coefficient of Rectangular antenna with inset and truncation on the Cylinder

The results (5.52-5.64 GHz) and (7.42-7.53 GHz) is satisfactory, but we need to increase the bandwidth. In this step, we'll change the dimensions of Trou Cylinder. Using the CST genetic optimization method, the optimization process will be run to obtain the best value for this dimension.

III.3.4.2.1 Effect of Length (Lcy)

In this case, we'll change the length(Lcy) from 3 to 5.75 mm while keeping the other parameters constant.

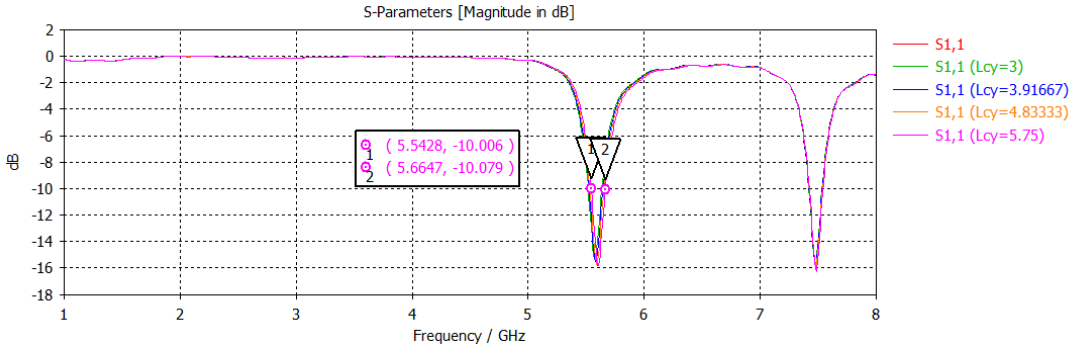

Figure III.22: Evolution of the reflection coefficient as a function of frequency for different lengths Lcy of Antenna with inset and Trou

The adaptation on the resonance frequencies(5.54-5.66GHz) is only affected by the variation of the truncation length.

III.3.4.2.2 Effect of Length (Lcy1)

In this case, we'll change the length (Lcy1) from 3 to 5 mm while keeping the other parameters constant.

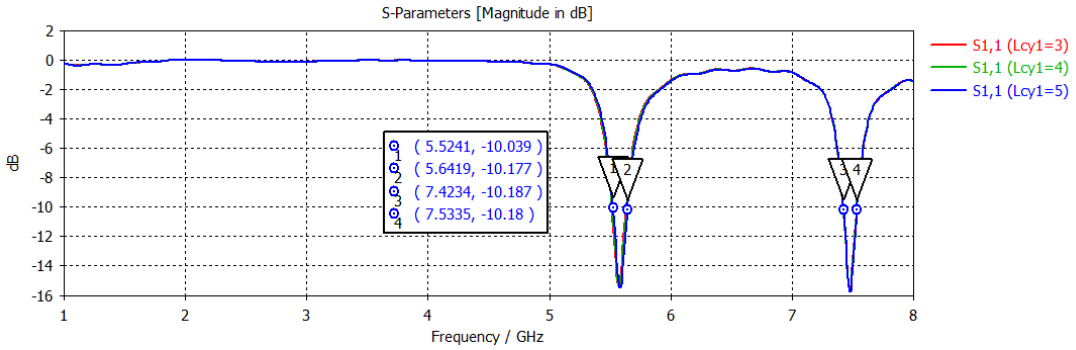

Figure III.23: Evolution of the reflection coefficient as a function of frequency for different lengths Lcy1 of Antenna with inset and Trou

The adaptation on the resonance frequencies(5.52-5.64GHz) and (7.42-7.53GHZ) is only affected by the variation of the truncation length.

III.4 Conclusion

In this chapter, we used the CST simulator to perform a parametric analysis of a printed lotus flower antenna. The goal of this investigation is to see how each parameter (radiating patch dimension, hole creation, and stub addition) affects the antenna's characteristics and performance, such as the reflection coefficient, adaptation, resonance frequency, and bandwidth.

Chapter IV
Design of a Reconfigurable EBG

IV.1 Introduction

We did an in-depth parametric research in the previous chapter that led to the values of the different dimensions of the antenna corresponding to the Wi-Fi apps. Diodes will be arranged in the structure of the patch to modify the resonance frequency by adjusting the state of these switching diodes to see the influence of reconfigurability on frequency operational of the antenna. In this chapter, reconfigurable antennas are used for wireless local area network (WLAN) applications according to the IEEE 802.11 standard. The resulting results must be tweaked to meet operational requirements.

Active components are used to drive reconfigurable antennas to change their characteristics (frequency operation, radiation pattern, and polarization) in a dynamic way (PIN diode, etc.). The complexity of the active components, the implementation of the activation circuits, and the difficulty of design, however, limit this reconfiguration. There is no perfect method for determining the antennae's arrangement. We'll start with a simple antenna and a single (existing antenna) to achieve reconfigurability, then add active components and resonant structures. The surface current distribution is plainly altered as a result of these enhancements, which changes the antenna radiation characteristics.

Our objective is to design an antenna that can operate on the WLAN spectrum (at 2.45 GHz). This same antenna can be reconfigured to operate on a different WLAN band after reconfiguration (at a frequency of 5.8 GHz). To attain this objective, we must optimize the antenna's specifications. Although optimization is not a new concept, it is frequently applied in a variety of industries. For example, in electronics, optimization is used to reduce the size of circuits and to provide the best possible combination of characteristics (reconfigurable antenna, multi-band antenna) and antenna parameters.

IV.2 Optimization Tool

IV.2.1 Definition

Optimization is the process of reducing or maximizing a cost function (objective). The optimization of a microstrip antenna entails precisely approximating one of some parameters, such as the resonance frequency, input impedance, or reflection coefficient S_{11}.

IV.2.2 Methods of optimization

There are many optimization methods used for antenna design. Among these optimization methods, stochastic methods like genetic algorithms and particle swarm optimization (PSO) can be mentioned, as well as analytical ones like Newton's method.

IV.2.2.1 Genetic Algorithms

The concept of natural selection, introduced by C. Darwin, is the inspiration for genetic algorithms (GA). Its principle is to model the evolution of an unsold item population by using various genetic operators (selection, crossover, and mutation), iteratively. When a population is selected based on a given cost function, the population tends to improve iteratively.

The advantages of genetic algorithms (GA) over traditional optimization approaches are numerous.

• It is capable of optimizing both real and binary variables.

• It does not necessitate the computation of a cost function's derivatives (semi-random).

• It can lead to a list of solutions if it can reach a global minimum without becoming locked in a local minimum.

The main disadvantage is the extremely sluggish convergence time.

IV.2.2.2 Quasi-Newton method

The quasi-Newton method is a method that is similar to Newton's method.

The quasi-Newton approach is based on Newton's method for determining the points stations of a function with a zero gradient. The idea behind it is to expand on Newton's iterative formula. The calculus of derivatives $f''(x_n)$. is required by Newton's approach. This is a drawback in practice because the function f does not always have an analytical expression.

IV.3 Modeling of PIN Diode

PIN diodes are one of the most common types of diodes used as switches in telecommunications applications. RF switching circuits use these diodes in a variety of ways. In photodiodes, the PIN structure is also very beneficial.

In 1952, the PIN diode was initially used as a low frequency high power rectifier. It was also utilized in a variety of microwave applications, though it wasn't until 1960 that this became increasingly common.

IV.3.1 Definition

A PIN diode (Positive Intrinsic Negative diode) is a semiconductor device with an undoped region (intrinsic region I) sandwiched between two additional sections doped with N and P types, respectively.

Figure IV.1 depicts a PIN switch's equivalent circuit, which may be turned on or off. The switch can be represented as a resistance and an inductance in the ON state (Figure IV.1.b). The diode will be mimicked in the OFF state by a capacitor in series with a resistor, all in series with an inductor, as shown in (Figure IV.1).

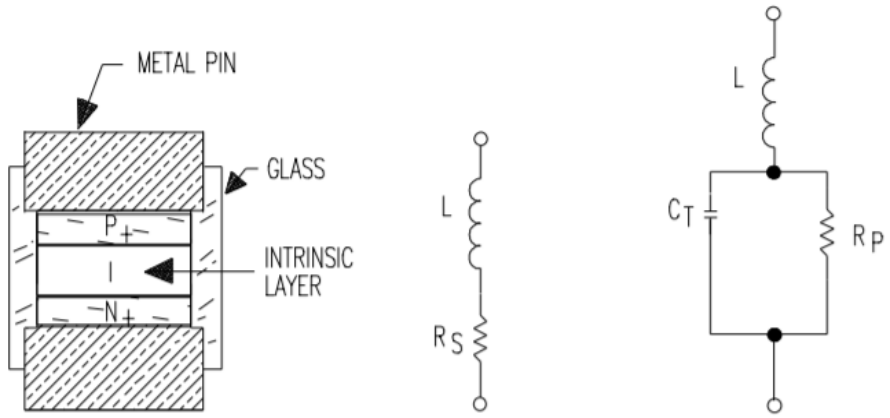

(a) (b) (c)

Figure IV.1: The equivalent circuit of the PIN diode: (a) Cross Section of Basic PIN Diode, (b) Forward Bias Equivalent Circuit (c) Reverse Bias Equivalent Circuit [30].

IV.3.2 Characteristics of PIN diodes

The PIN diode has a number of qualities that distinguish it from other diodes.

• The high frequency resistance is inversely related to the DC bias current across the diode, among other significant features. The PIN diode acts as a variable resistor in direct

polarization. This high frequency resistance can be anything between 0.1 and 10 k. The useful range is sometimes smaller.

• PIN diodes have a significant reverse breakdown characteristic thanks to the intrinsic layer's large depletion layer.

• The PIN diode can be utilized for amplitude modulation of an RF signal when the control current is alternatively varied.

• The diode has a fast switching time (less than 100 ns)

IV.3.3 The Advantages and Desadvantages of a PIN diode

PIN diode, like all other switches, has various advantages and cons.

a) Advantages

• A high-voltage rectifier can be made out of a PIN diode.

• Because of the great distance between the P and N areas, the intrinsic region provides a high separation between the P and N regions, allowing higher reverse voltages to be tolerated during reverse bias. A PIN diode can be thought of as an ideal RF switch.

• Because light is converted into current within a photodiode's depletion region, extending the depletion region by adding an intrinsic layer enhances performance.

b) Desadvantages

•The biggest disadvantage of a PIN diode is its recovery time (from state ON to state OFF).

• PIN diodes have power losses due to the reverse recovery time.

IV.3.4 Diode PIN (BAR50-02)

RF-MEMS, Varactors, and PIN diode were among the technologies and switches described previously for reconfiguration

The BAR50-02V is an Infineon technology PIN Diode. It's a single-pole, single-throw system (SPST). As shown in Figure IV.2, the SPST switch has one input and one output port. The frequency range of this diode is 10 MHz to 6 GHz, and the insertion loss is 0.27 to 0.56 dB. 12 to 24.5 dB isolation, 0.95 to 1.1 V forward voltage, 100 mA forward current, and 1100 ns recovery time

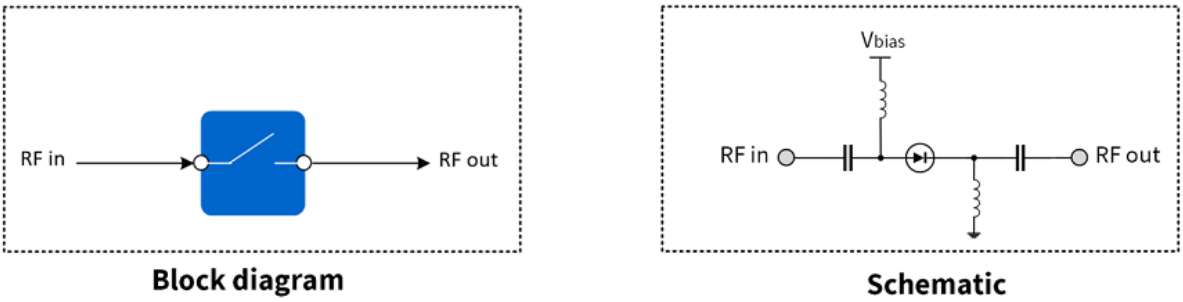

Figure IV.2: schematic of SPST switch: PIN diode (BAR50-02)

I.V.4 A frequency-reconfigurable antenna design

After a parametric study and optimization, we will construct a frequency-configurable antenna utilizing PIN diodes. To obtain the proper resonance frequency, we must find the right modification of these factors. The purpose of an antenna patch is to optimize certain of the antenna's attributes in order to achieve the desired qualities in terms of resonant frequency and matching. This reversible antenna can transmit on either the 2.4GHz or 5.8GHz bands. WLAN applications are limited to these two bands. The following steps must be followed in order to optimize using the CST Microwave studio simulator.

We'll start by selecting the *Optimizer* symbol from the simulation menu, and then tick (choose).

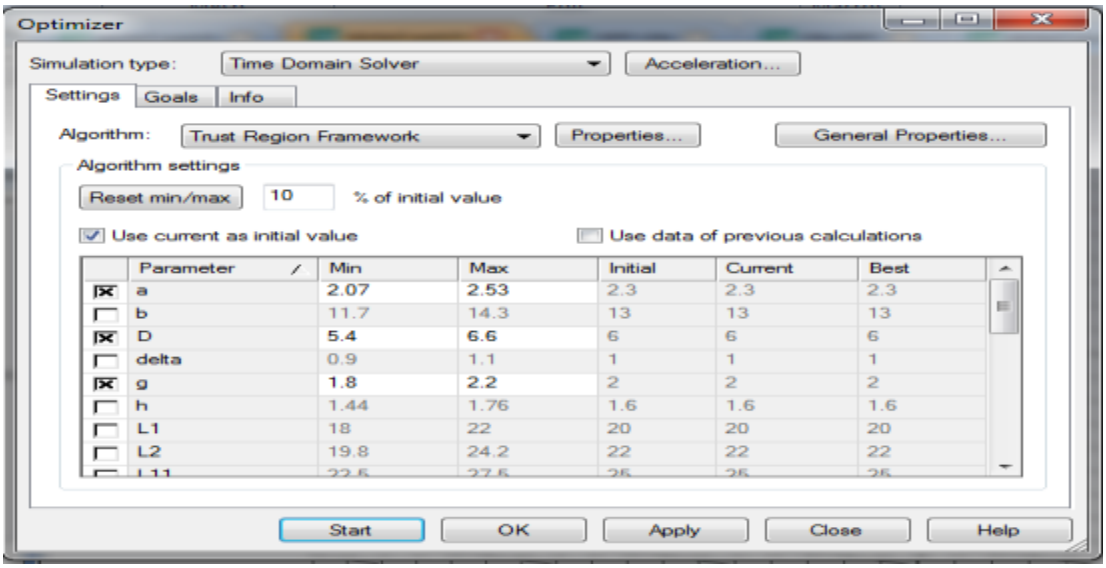

Figure IV.3: Optimization parameter selection

Second, we'll defind the goal. In our case, the coefficient of reflection S11 in the WLAN 1 range must be less than -10 dB. (around 2.45 GHz). WLAN band 2 is no exception (around 5.8 GHz).

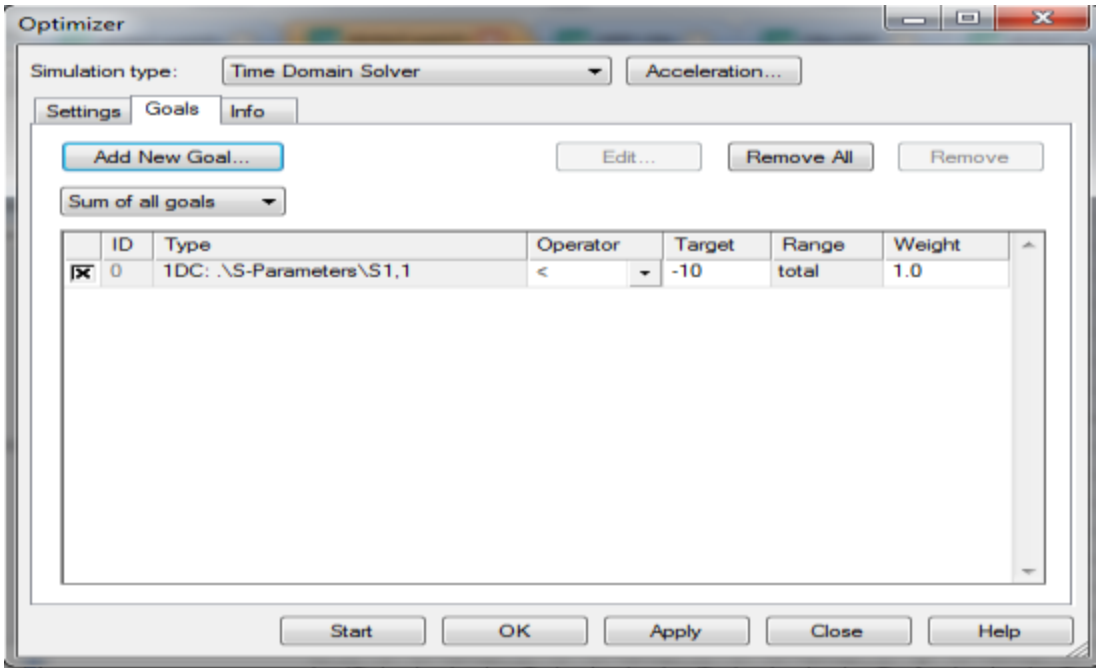

Figure IV.4: The objective's definition (Goal)

IV.4.1 The proposed antenna geometry

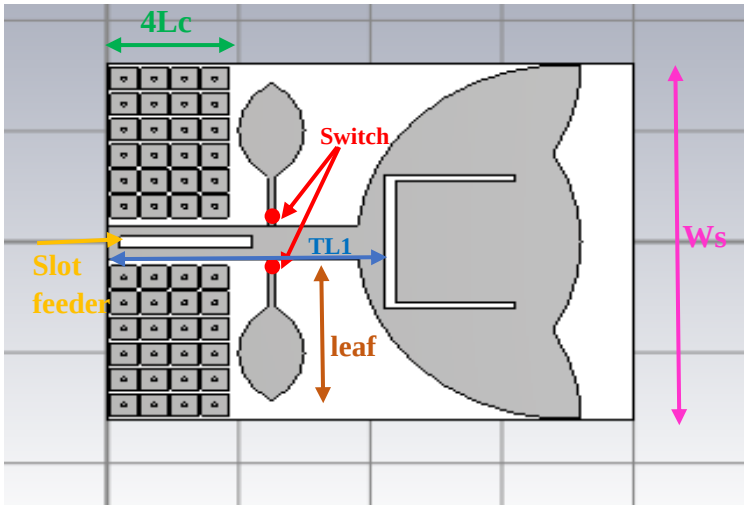

(a)

Lgnd

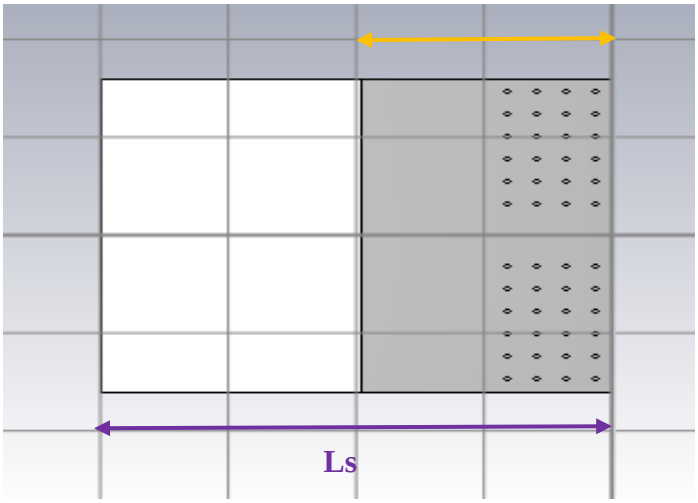

(b)

FigureIV.5: The antenna's planned geometry;
(a) front view,(b) back view

In the table below, the best settings are listed

Table IV.1: The dimensions in millimeter of the proposed antenna

Parameter	Lgnd	Wgnd	Ls	Wf	L1	R1	Lc	X1	Rleaf	Lslot
Value(mm)	25	32	40	3	25	9	1.5	19	2.6	20

To make the antenna reconfigurable in frequency, we will place PIN diodes, which will take two states (ON, OFF), in the structure.

❖ **The PIN diode is modeled**

The PIN diode has two states: ON and OFF, as you may know. To make our task easier, we'll model the ON state with a piece of metal. A discontinuity is used to represent the OFF state (without metal).

IV.5 The simulation results

To run the simulation, we'll use two diodes, giving us four different scenarios to choose from (ON-ON, OFF-OFF, OFF-ON, ON-OFF)

The two diodes (models) are put between the feeder and the leaf on both sides (which affects the antenna adaptation).

❖ State 1: OFF-OFF

In this case, the diodes are modeled by discontinuities (without metal) at the antenna structure, therefore the space between the food line and the stub considered as A slit that will influence the adaptation of the antenna.

Because the diodes are depicted as discontinuities (without metal) at the antenna construction in this scenario, the space between the feed line and the leaf is regarded as a slit that will affect the antenna's adaption.

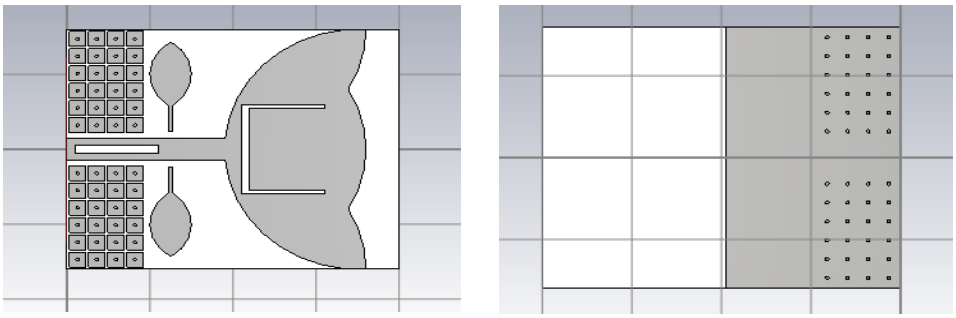

FigureIV.6: the antenna structure on the state OFF-OFF; front view

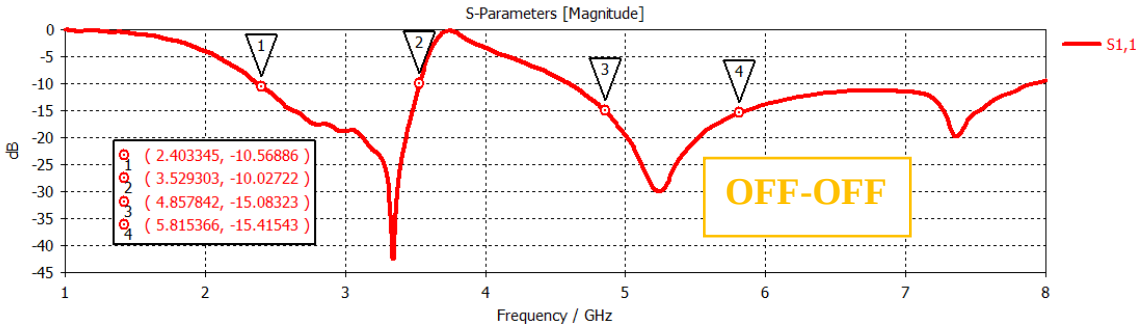

FigureIV.7: The reflection coefficient of the state OFF-OFF

This reconfiguration allows an echo to be obtained at a frequency of 2.4GHz, which is very useful. This band corresponds to the WLAN band.

The adaptation is adequate in the first result (2.40GHz-3.52GHz) (S11 is about -42). Also in the second result (4.85GHz-5.81GHz) for the frequency of 5.8GHz;(S11 is about -30).

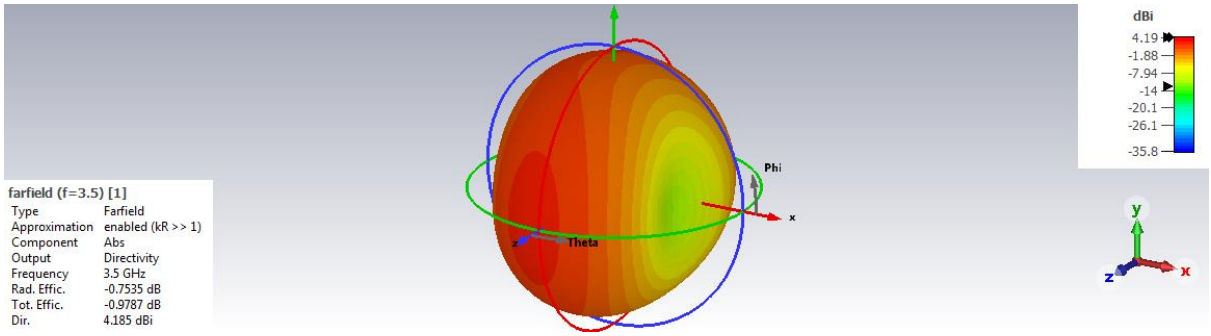

FigureIV.8: The radiation pattern for the 3.5GHz frequency (3D)

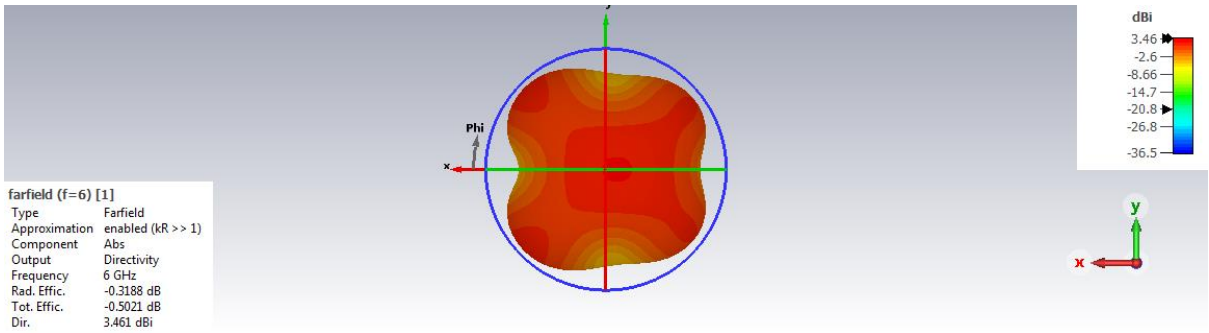

FigureIV.9: The radiation pattern for the 3.5GHz frequency (3D)

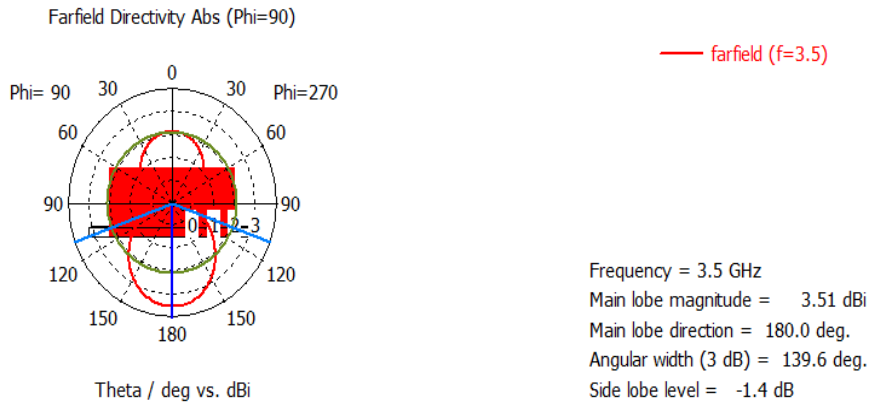

FigureIV.9: The radiation pattern for the 3.5GHz frequency on plane Phi=90°(2D)

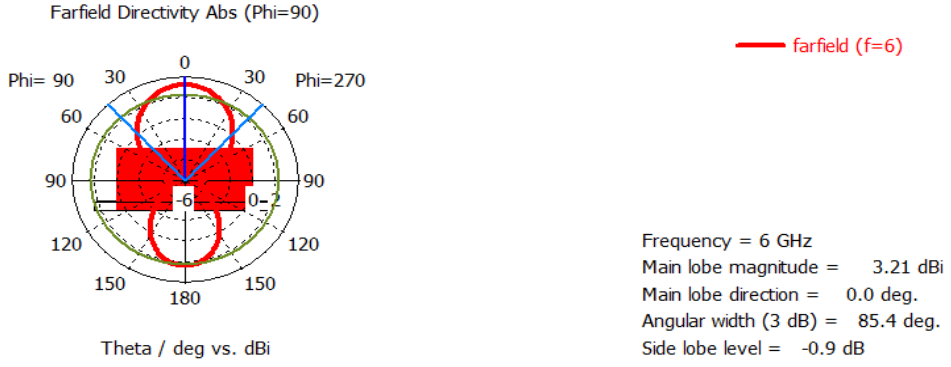

FigureIV.10: The radiation pattern for the 6GHz frequency on plane Phi=90°(2D)

We show the normalized far field radiation pattern in 3D at the frequency f = 3.5 GHz. And at the frequency f=6GHz. At f=3.5 GHz, the maximum overall realized gain is on the order of 3.51 dBi., At f=6 GHz, the maximum overall realized gain is on the order of 3.21 dBi. As shown in FiguresIV. (9,10), these radiation diagrams have been reproduced in 2D in the two planes phi=90° and phi=270°.

❖ State 2: ON-ON

In this case, we'll add two metal diodes to connect the leaf to the feed line; the antenna's structure, as well as the distribution of surface current on the patch, will be altered.

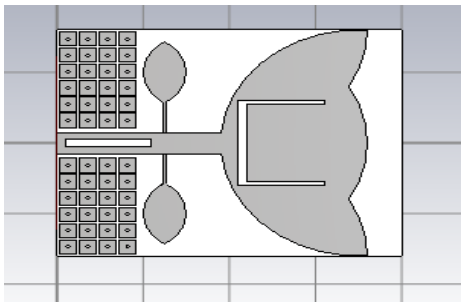

FigureIV.11: the antenna structure on the state ON-ON; front view

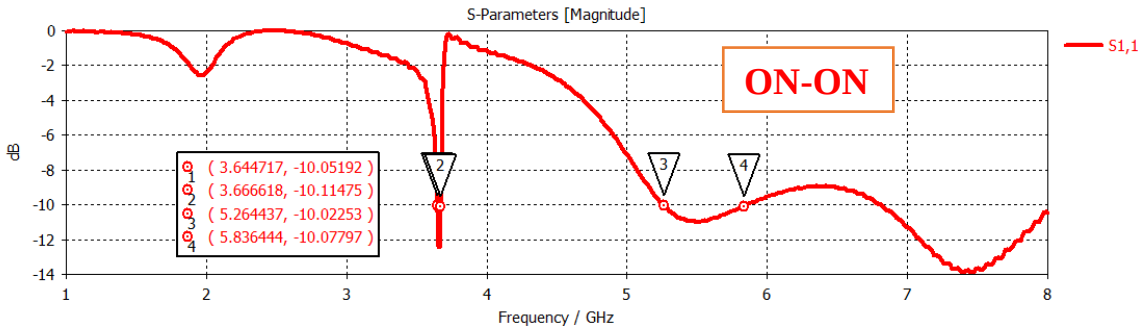

FigureIV.12: The reflection coefficient of the state ON-ON

The first result (3.54GHz-3.66GHz) (S11<= -12); the adaptation is adequate. The second result (5.26GHz-5.83GHz) for the frequency of 5.8GHz; the adaptation not adequate (S11<= -11dB).

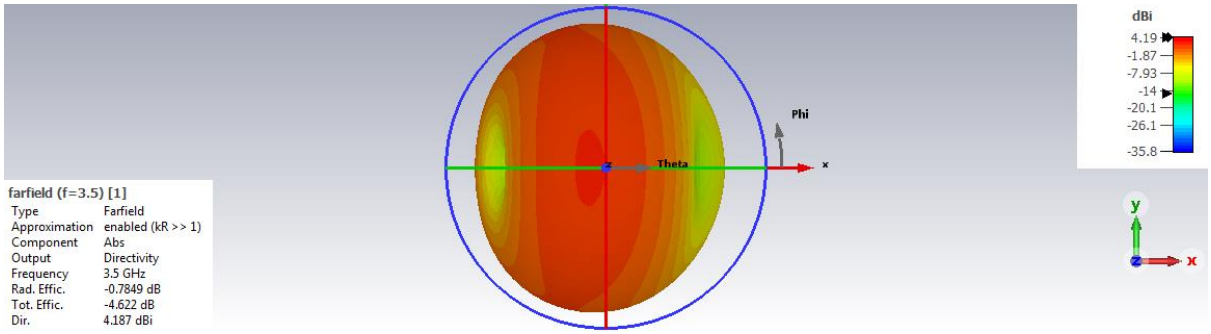

FigureIV.13: The radiation pattern for the 3.5GHz frequency (3D)

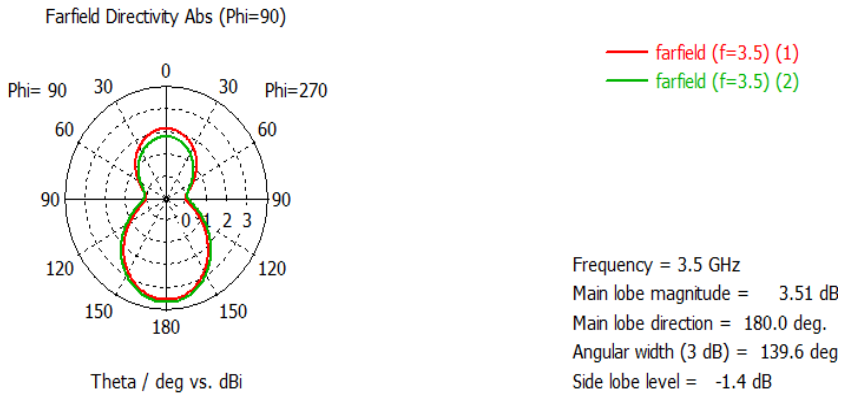

FigureIV.14: The radiation pattern for the 3.5GHz frequency on plane Phi=90°(2D)

We show the normalized far field radiation pattern in 3D at the frequency f = 3.5 GHz. At f=3.5 GHz, the maximum overall realized gain is on the order of 3.51 dBi., As shown in FiguresIV.14, these radiation diagrams have been reproduced in 2D in the two planes phi=90° and phi=270°.

❖ State 3: OFF-ON

In this version of the antenna, we will add a single diode on one of the two sides to connect the supply line with the leaf. The second side is considered a slot.

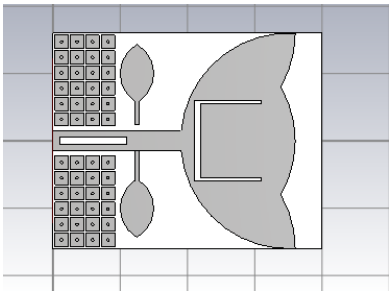

FigureIV.15: the antenna structure on the state OFF-ON; front view

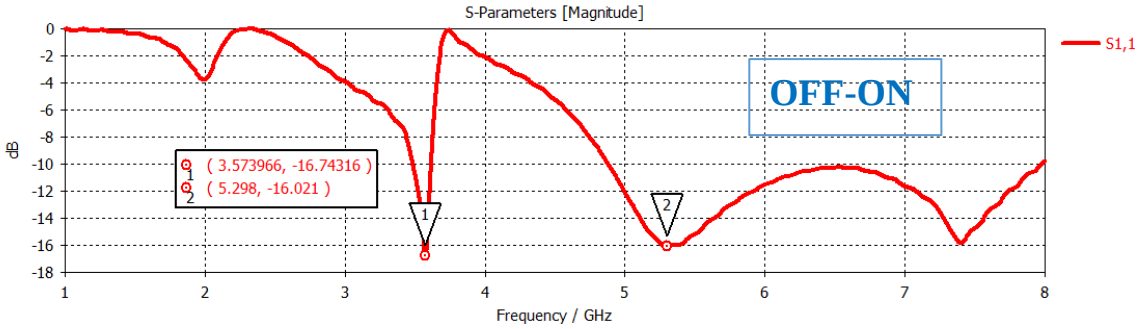

FigureIV.16: The reflection coefficient of the state OFF-ON

With this reconfiguration, you can have two resonance frequencies, one at (3.57GHz) with a -16 dB adaptation. And one at (5.29GHz) with a -16 dB adaptation for the frequency 5.8GHz.

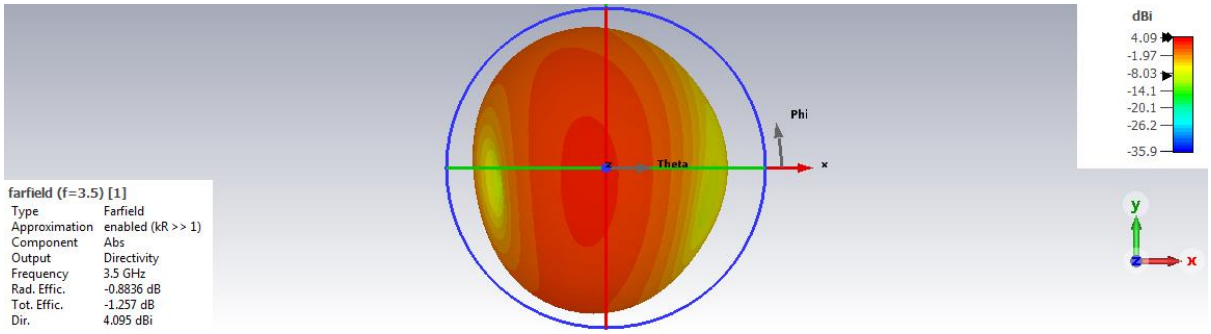

FigureIV.17: The radiation pattern for the 3.5GHz frequency (3D)

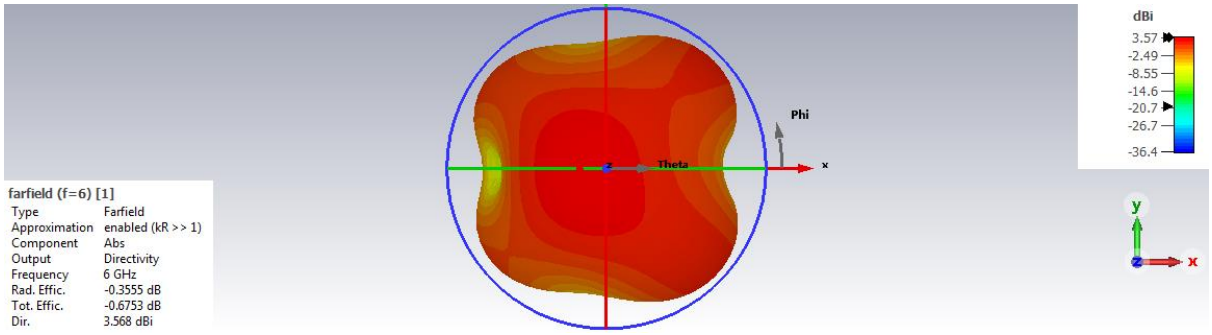

FigureIV.18: The radiation pattern for the 6GHz frequency (3D)

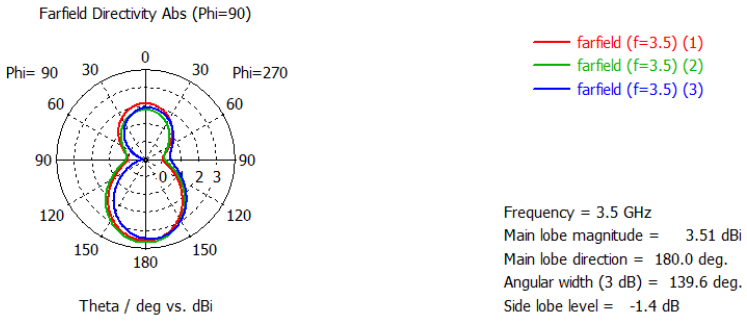

FigureIV.19: The radiation pattern for the 3.5GHz frequency on plane Phi=90°(2D)

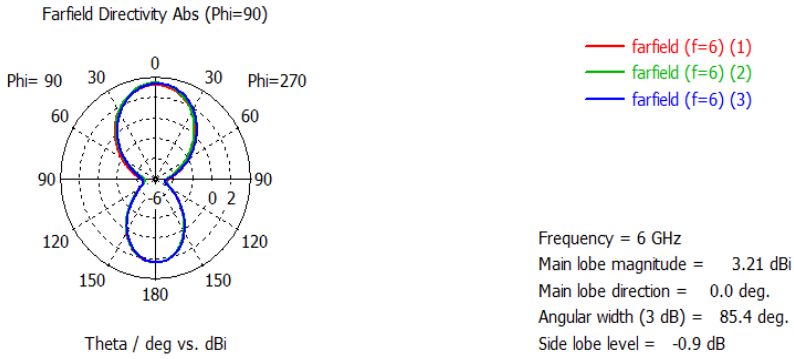

FigureIV.20: The radiation pattern for the 6GHz frequency on plane Phi=90°(2D)

We show the normalized far field radiation pattern in 3D at the frequency f = 3.5 GHz. And at the frequency f=6GHz. At f=3.5 GHz, the maximum overall realized gain is on the order of 3.51 dBi., At f=6GHz, the maximum overall realized gain is on the order of 3.21 dBi. As shown in FiguresIV. (19,20), these radiation diagrams have been reproduced in 2D in the two planes phi=90° and phi=270°.

❖ State 4: ON-OFF

In this version of the antenna, we will add a single diode on one of the two sides to connect the supply line with the leaf. The second side is considered a slot.

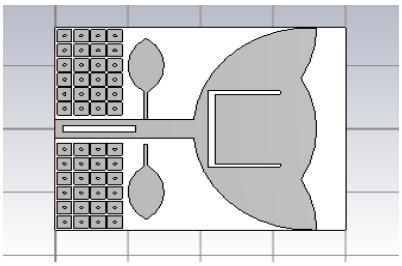

FigureIV.21: The antenna structure on the state ON-OFF; front view

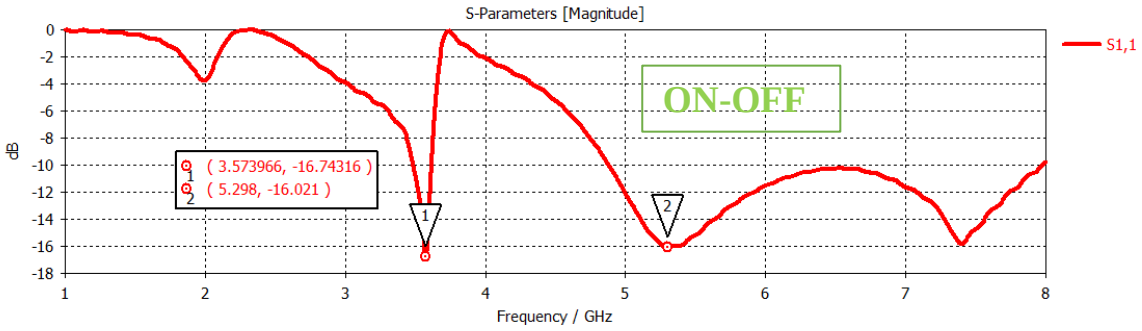

FigureIV.22: The reflection coefficient of the state ON-OFF

With this reconfiguration, you can have two resonance frequencies, one at (3.57GHz) with a -16 dB adaptation. And one at (5.29GHz) with a -16 dB adaptation for the frequency 5.8GHz.

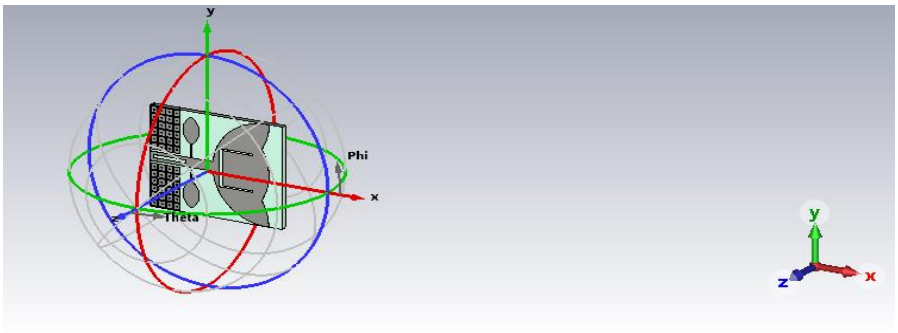

FigureIV.23: The radiation pattern Excitation(3D)

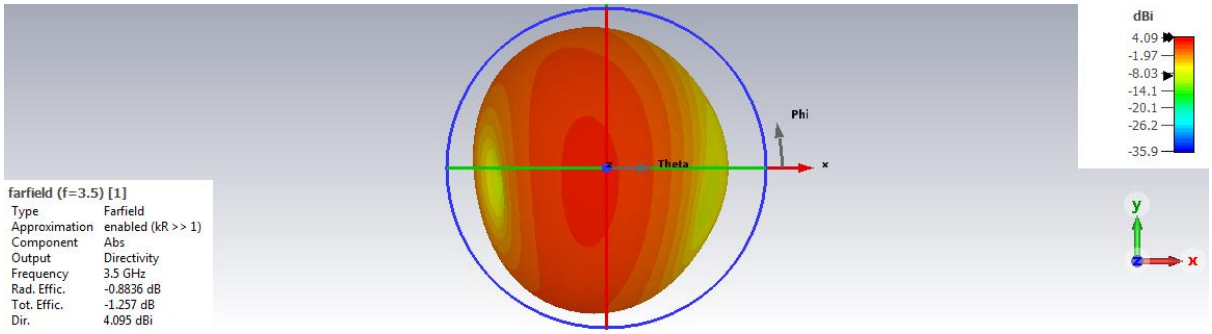

FigureIV.24: The radiation pattern for the 3.5GHz frequency (3D)

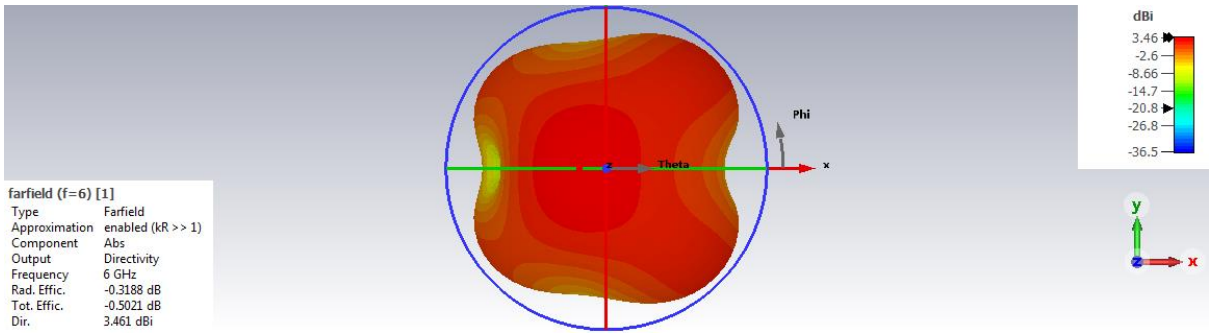

FigureIV.25: The radiation pattern for the 6GHz frequency (3D)

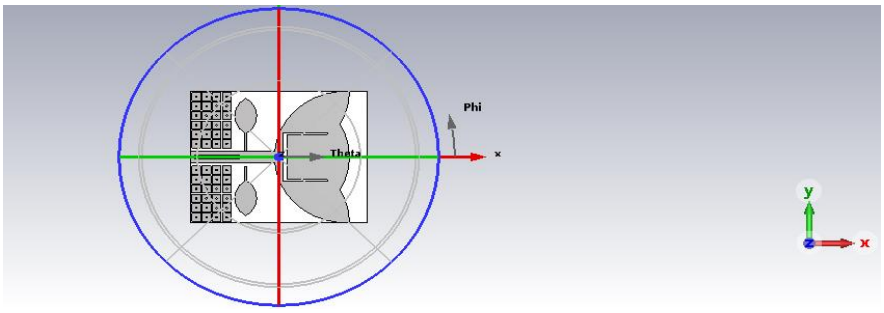

FigureIV.26: The radiation pattern Excitation(3D)

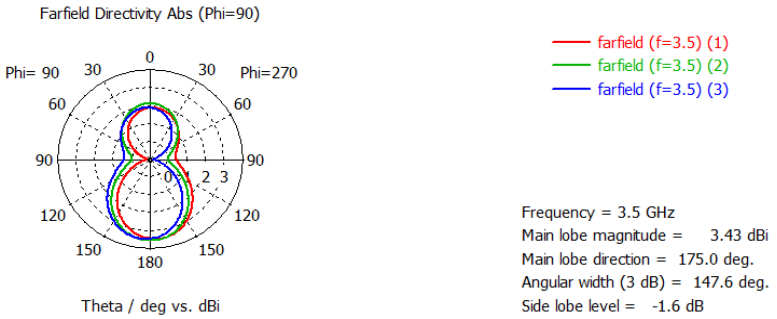

FigureIV.27: The radiation pattern for the 3.5GHz frequency on plane Phi=90°(2D)

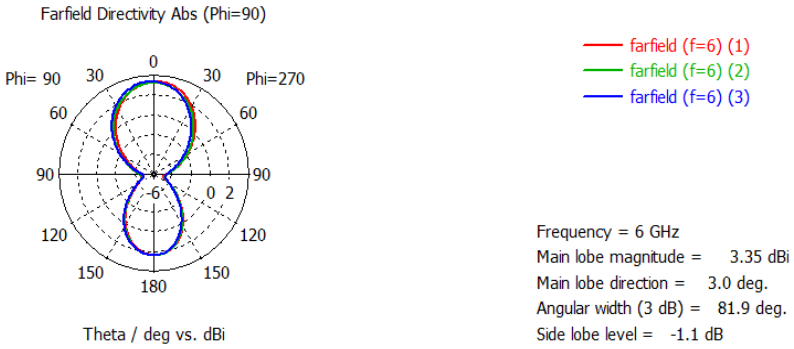

FigureIV.28: The radiation pattern for the 6GHz frequency on plane Phi=90°(2D)

We show the normalized far field radiation pattern in 3D at the frequency f = 3.5 GHz. And at the frequency f=6GHz. At f=3.5 GHz, the maximum overall realized gain is on the order of 3.43 dBi., At f=6GHz, the maximum overall realized gain is on the order of 3.35 dBi. As shown in FiguresIV. (27,28), these radiation diagrams have been reproduced in 2D in the two planes phi=90° and phi=270°.

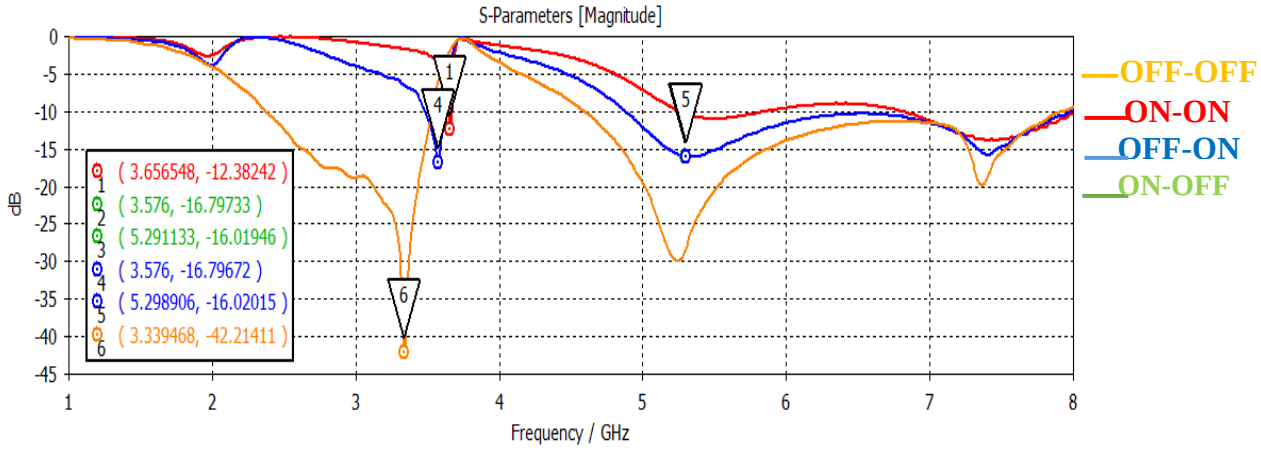

FigureIV.29: The reflection coefficient as a function of frequency for the different cases Possible

Table IV.2: The results of different possible cases

	Resonance Frequencie(GHz)	Reflexion Coefficient (dB)	Bandwidth(GHz)
OFF-OFF	3.33 GHz	-42.21 dB	(2.40GHz-3.52GHz)
ON-ON	3.65 GHz	-12.38 dB	(3.54GHz-3.66GHz)
ON-ON	5.24 GHz	-29.93 dB	(4.8GHz-5.8GHz)
OFF-ON	3.57 GHz	-16.79 dB	(3.57GHz-5.8GHz)
ON-OFF	3.57 GHz	-16.79 dB	(3.57GHz-5.8GHz)

With strong antenna matching and limited bandwidth in WLAN applications, the reconfigurability is well confirmed, as shown in this table.

We can see that the reconfigurability effect allows us to switch between different frequencies without changing the antenna; for example, if you want to go through different services of the WLAN application, you can easily do so thanks to reconfigurable antennas.

IV.6 Conclusion

Chapter 4 presents the design of a frequency reconfigurable antenna.

The proposed antenna that we made is reached after, an in-depth parametric study and then optimization that allows us to adjust a few parameters in order to achieve our desired results. reconfigurability is achieved using active components featured in the PIN diode which was modeled by a simple metal piece for the on-state and a discontinuity for the blocked state. Reconfigurable antenna can switch between two frequency bands (2.4 and 5.8 GHz). These two bands are dedicated to WLAN applications.

Conclusions

Conclustion

We have chosen to study reconfigurable antennas for their obvious importance in many telecommunications systems

In this thesis, we have studied some points to design a reconfigurable antenna with EBG strcture. Active components like as PIN diodes enable reconfigurable antennas to switch between their capabilities.

The objective of our work was the design of a reconfigurable antenna in frequency that allows switching between two bands (2.4GHz and 5.8GHz) and (3.5 to 6GHz) dedicated to WiFi apps. To achieve this objective, a parametric study was made using the 3D electromagnetic simulator CST studio 2021 in the time domain. This full-wave simulator is based on the resolution of the maxwell equation using the finite integration method. This software is used to model PIN diodes (packages) in the two ON/OFF states under the design studio interface.

During this work, we developed a reconfigurable antenna from of a simple lotus antenna using an in-depth parametric study that allowed us to have a great idea about the effect of each parameter on the characteristics antennas such as reflection coefficient, resonant frequency and bandwidth. an optimization process was run using the integrated genetic algorithm in the CST software. The reconfigurable antenna was designed with a trou leaf in the two sides of the patch by adding a slots. For the reconfigurability, Two PIN-diodes are used between th trou leaf and the patch (feed line) on two sides.

In fact, switching the resonance frequency from one WLAN 1 band to another WLAN 2 band is achievable thanks to the usage of PIN diodes (metallic versions).

We tried to employ PIN-diode (BAR 50-02V) in this investigation because it works in the frequency range [1-6 GHz].

References

References

[1] Yang, S. -L. S., A. Kishk, and K. -F. Lee, "Frequency Reconfigurable U-Slot Microstrip Patch Antenna," *IEEE Antennas and Wireless Propagation Letters*, Vol. 7, 2008, pp. 127 130.

[2] Islam, M. R., and M. Ali, "Switched Parasitic Body-Worn Array for High Data Rate Wireless Applications," *IEEE Antennas and Wireless Propagation Letters*, Vol. 11, 2012, pp. 693–696.

[3] Qin, P. -Y., et al., "A Reconfigurable Antenna with Frequency and Polarization Agility," *IEEE Antennas and Wireless Propagation Letters*, Vol. 10, January 2011, pp. 1373–1376.

[4] Bernhard, J. T., "Reconfigurable Antennas," in *Antenna Engineering Handbook*, 4th ed., J.Volakis, (ed.), New York: McGraw-Hill, 2007.

[5] N. O. Parchi, H. J. Basherlou, Y. I. A. Al-Yasir, R. A. Abd- Alhameed, A. M. Abdulkhaleq J. M. Noras., "Recent Developments of Reconfigurable Antennas for Current and Future Wireless Communication Systems", *Electronics*, Vol. 128, pp. 1-17, 2019.

[6] Reconfigurable Antennas with Single and Multiple Reconfigurability Functions for Wireless Communications Md. Shahidul Alam B.Sc. (Electrical and Electronic Engg.), M. Sc. (Electrical, Electronic and System Eng).

[7] Kamariah Binti Ismail. Nur Syuhada Binti Khairul Shamsudin Fractal Antenna with Electromagnetic Band Gap (EBG) Structure for Wireless Application.

[8] Antenna Masoumeh. Rezaei Abkenar Pejman Rezaei. EBG Structures Properties and their Application to Improve Radiation of a Low Profile.

[9] IEEE Press Editorial Board. Electromagnetic Bandgap (EBG) Structures.

[10] Mémoire Chaima Amel. Etude et conception d'une antenne reconfigurable pour les applications WLAN.

[11] Mémoire kawkach madjed, Saadallah ali. study and design of a reconfigurable antenna using defective ground structure for mobile communication.

الملخص

من أجل مواكبة متطلبات الأنظمة الخلوية الحديثة المشار إليها في الحاجة إلى دعم تطبيقات المجال الواسع، تعتبر الهوائيات من أكثر القطاعات التي تشهد تقدمًا استثنائيًا واهتمامًا متزايدًا في الوقت الحالي. نتيجة لذلك، ظهرت هوائيات تدعم نطاق تردد واسع

خلال هذا العمل، طورنا هوائيًا قابلًا لإعادة التكوين من هوائي لوتس بسيط باستخدام دراسة بارامترية متعمقة سمحت لنا بالحصول على فكرة رائعة عن تأثير كل معلمة على خصائص الهوائيات مثل معامل الانعكاس وتردد الرنين وعرض النطاق الترددي. تم تصميم الهوائي القابل لإعادة التشكيل بورق شجر في جانبي الرقعة بإضافة فتحات. لإعادة ثنائية بين ورقة شجر والرقعة (خط التغذية) على الجانبين. تم تشغيل PIN التكوين، يتم استخدام اثنين من صمامات عملية التحسين باستخدام الخوارزمية الجينية المتكاملة في برنامجCST.

الكلمات المفتاحية: هوائي قابل لإعادة التشكيل ، ورقة نباتية ، لوتس، شريحة الارضي،

CST، microstrip patch

Abstract

In order to stay up with the requirements of modern cellular systems indicated in the need to support wide-field applications, antennas are regarded the most sectors that are witnessing extraordinary progress and increasing attention in the current moment. As a result, antennas that support a wide frequency range have emerged.

During this work, we developed a reconfigurable antenna from of a simple lotus antenna using an in-depth parametric study that allowed us to have a great idea about the effect of each parameter on the characteristics antennas such as reflection coefficient, resonant frequency and bandwidth. The reconfigurable antenna was designed with a trou leaf in the two sides of the patch by adding a slots. For the reconfigurability, Two PIN-diodes are used between th trou leaf and the patch (feed line) on two sides. an optimization process was run using the integrated genetic algorithm in the CST software.

Key words: Reconfigurable, microstrip patch antenna, CST, trou leaf, lotus, ground

Résumé

Afin de répondre aux exigences des systèmes cellulaires modernes indiquées dans la nécessité de prendre en charge les applications à large champ, les antennes sont considérées comme les secteurs les plus témoins de progrès extraordinaires et d'une attention croissante à l'heure actuelle. En conséquence, des antennes prenant en charge une large gamme de fréquences ont vu le jour.

Au cours de ce travail, nous avons développé une antenne reconfigurable à partir d'une simple antenne lotus en utilisant une étude paramétrique approfondie qui nous a permis d'avoir une bonne idée de l'effet de chaque paramètre sur les caractéristiques des antennes telles que le coefficient de réflexion, la fréquence de résonance et la bande passante. L'antenne reconfigurable a été conçue avec une feuille de trou dans les deux côtés du patch en ajoutant des fentes. Pour la reconfigurabilité, deux diodes PIN sont utilisées entre la feuille de trou et le patch (ligne d'alimentation) des deux côtés. Un processus d'optimisation a été exécuté à l'aide de l'algorithme génétique intégré dans le logiciel CST.

Mots clés : Reconfigurable, antenne patch microstrip, CST, trou leaf, lotus, la masse.